relationship to cardiovascular risk factors: the Insulin Resistance Atherosclerosis Study. Diabetes Care 1999;22:562-8.

[8] Fukushima M, Usami M, Ikeda M, Nakai Y, Taniguchi A, Suzuki H, et al. Insulin secretion and insulin sensitivity at different stages of glucose tolerance: a cross-sectional study of Japanese type 2 diabetes. Metabolism 2004;53:831-5.

[9] Taniguchi A, Fukushima M, Sakai M, Kataoka K, Nagata I, Doi K, et al. The role of the body mass index and triglyceride levels in identifying insulin-sensitive and insulin-resistant variants in Japanese non insulin-dependent diabetic patients. Metabolism 2000;49:1001-5.

[10] Taniguchi A, Fukushima M, Sakai M, Miwa K, Makita T, Nagata I, et al. Remnant-like particle cholesterol, triglycerides, and insulin resistance in nonobese Japanese type 2 diabetic patients. Diabetes Care 2000;23:1766-9.

[11] Yatagai T, Nagasaka S, Fukushima M, Taniguchi A, Nakamura T, Kuroe A, et al. Hypoadiponectinemia is associated with visceral fat accumulation and insulin resistance in subjects with type 2 diabetes mellitus. Metabolism 2003;52:1274-8.

[12] Okumura T, Taniguchi A, Nagasaka S, Sakai M, Fukushima M, Kuroe A, et al. Relationship of regional adiposity to serum leptin level in nonobese Japanese type 2 diabetic male patients. Diabetes Metab 2003;29:15-8.

[13] Taniguchi A, Nakai Y, Sakai M, Yoshii S, Hamanaka D, Hatae Y, et al. Relationship of regional adiposity to insulin resistance and serum triglyceride levels in nonobese Japanese type 2 diabetic patients. Metabolism 2002;51:544-8.

[14] Fontbonne A, Eschwege E, Cambien F, Richard JL, Ducimetiere P, Thibult N, et al. Hypertriglyceridaemia as a risk factor of coronary heart disease mortality in subjects with impaired glucose tolerance or diabetes: results from the 11-year follow-up of the Paris Prospective Study. Diabetologia 1989;32:300-4.

[15] Shinada K, Miyazaki T, Daida H. Adiponectin and atherosclerotic disease. Clin Chim Acta 2004;344:1-12.

[16] Wallace AM, McMahon AD, Packard CJ, MIBiol AK, Shepherd J, et al. Plasma leptin and the risk of cardiovascular disease in the West of Scotland Coronary Prevention Study (WOSCOPS). Circulation 2001;104:3052-6.

[17] Isomaa B, Almgren P, Tuomi T, Forsen B, Lahti K, Nissen M, et al. Cardiovascular morbidity and mortality associated with the metabolic syndrome. Diabetes Care 2002;24:683-9.

[18] Pouliot MC, Despres JP, Lemieux S, Moorjani S, Bouchard C, Tremblay A, et al. Waist circumference and abdominal sagittal diameter: best simple anthropometric indexes of abdominal visceral adipose tissue accumulation and related cardiovascular risk in men and women. Am J Cardiol 1994;73:460-8.

[19] World Health Organization. Diabetes mellitus: report of a WHO study group. Geneva: World Health Org; 1985 [Tech. Rep. Ser., no. 727].

[20] Ohya M, Taniguchi A, Fukushima M, Nakai Y, Kawasaki Y, Nagasaka S, et al. Three measures of tumor necrosis factor-alpha activity and insulin resistance in non-obese Japanese type 2 diabetic patients. Metabolism 2005;54:1297-301.

[21] Matthews DR, Hosker JP, Rudenski AS, Naylor BA, Treacher DF, Turner RC. Homeostasis model assessment: insulin resistance and B-cell function from fasting plasma glucose and insulin concentrations in man. Diabetologia 1985;28:412-9.

[22] Bonora E, Targher G, Alberiche M, Bonadonna RC, Saggiani F, Zenere M, et al. Homeostasis model assessment closely mirrors the glucose clamp technique in the assessment of insulin sensitivity. Diabetes Care 2000;23:57-63.

[23] Emoto M, Nishizawa Y, Maekawa K, Hiura Y, Kanda H, Kawagichi T, et al. Homeostasis model assessment as a clinical index of insulin resistance in type 2 diabetic patients treated with sulfonylureas. Diabetes Care 1999;22:818-22.

[24] Taniguchi A, Nishimura F, Murayama Y, Nagasaka S, Fukushima M, Sakai M, et al. *Porphyromonas gingivalis* infection is associated with carotid atherosclerosis in non-obese Japanese type 2 diabetic patients. Metabolism 2003;52:142-5.

[25] Chaiken RL, Banerji MA, Pasmantier RM, Huey H, Hirsch S, Lebovitz HE. Patterns of glucose and lipid abnormalities in black NIDDM subject. Diabetes Care 1991;14:1036-42.

[26] Fujimoto WY, Bergstrom RW, Boyko EJ, Chen K-W, Leonetti DL, Newell-Morris L, et al. Visceral adiposity and incident coronary heart disease in Japanese-American men. The 10-year follow-up results of the Seattle Japanese-American Community Diabetes Study. Diabetes Care 1999;22:1808-12.

[27] Guha M, Bai W, Nadler J, Natarajan BR. Molecular mechanisms of alpha gene expression in monocytic cells via hyperglycemia-induced oxidant stress dependent and independent pathways. J Biol Chem 2000;275:17728-35.

[28] Shai I, Schulze MB, Manson JE, Rexrode KM, Stampfer MJ, Mantzoros C, et al. A prospective study of soluble tumor necrosis factor-α receptor II (sTNF-RII) and risk of coronary heart disease among women with type 2 diabetes. Diabetes Care 2005;28: 1376-82.

[29] Rauchhaus M, Doehner W, Francis DP, Davos C, Kemp M, Liebenthal C, et al. Plasma cytokine parameters and mortality in patients with chronic heart failure. Circulation 2000;102:3060-7.

[30] Kawasaki Y, Taniguchi A, Fukushima M, Nakai Y, Kuroe A, Ohya M, et al. Soluble TNF receptors and albuminuria in non-obese Japanese type 2 diabetic patients. Horm Metab Res 2005;37:617-21.

[31] Bruno G, Merletti F, Biggeri A, Bargero G, Ferrero S, Runzo C, et al. Metabolic syndrome as a predictor of all-cause and cardiovascular mortality in type 2 diabetes. The Casale Monferrato Study. Diabetes Care 2004;27:2689-94.

[32] Kahn R, Buse J, Ferrannini E, Stern M. The metabolic syndrome: time for a critical appraisal. Joint statement from the American Diabetes Association and the European Association for the study of diabetes. Diabetes Care 2005;28:2289-304.

Available online at www.sciencedirect.com
ScienceDirect
ELSEVIER
Biochemical and Biophysical Research Communications 364 (2007) 175–180
BBRC
www.elsevier.com/locate/ybbrc

Genetic inactivation of GIP signaling reverses aging-associated insulin resistance through body composition changes

Chizumi Yamada [a], Yuichiro Yamada [a,b,*], Katsushi Tsukiyama [a,1], Kotaro Yamada [a], Shunsuke Yamane [a], Norio Harada [a], Kazumasa Miyawaki [c], Yutaka Seino [a,d], Nobuya Inagaki [a,e]

[a] *Department of Diabetes and Clinical Nutrition, Kyoto University Graduate School of Medicine, 54 Shogoin-Kawahara-cho, Sakyo-ku, Kyoto 606-8507, Japan*
[b] *Department of Internal Medicine, Division of Endocrinology, Diabetes and Geriatric Medicine, Akita University School of Medicine, Akita, Japan*
[c] *Department of Experimental Therapeutics, Translational Research Center, Kyoto University Hospital, Kyoto, Japan*
[d] *Kansai Electric Power Hospital, Osaka, Japan*
[e] *CREST of Japan Science and Technology Cooperation (JST), Kyoto, Japan*

Received 5 September 2007
Available online 9 October 2007

Abstract

Aging is associated with increased fat mass and decreased lean mass, which is strongly associated with the development of insulin resistance. Gastric inhibitory polypeptide (GIP) is known to promote efficient storage of ingested nutrients into adipose tissue; we examined aging-associated changes in body composition using 10-week-old and 50-week-old wild-type (WT) and GIP receptor knockout ($Gipr^{-/-}$) mice on a normal diet, which show no difference in body weight. We found that $Gipr^{-/-}$ mice showed significantly reduced fat mass without reduction of lean mass or food intake, while WT mice showed increased fat mass and decreased lean mass associated with aging. Moreover, aged $Gipr^{-/-}$ mice showed improved insulin sensitivity, which is associated with amelioration in glucose tolerance, higher plasma adiponectin levels, and increased spontaneous physical activity. We therefore conclude that genetic inactivation of GIP signaling can prevent the development of aging-associated insulin resistance through body composition changes.

Keywords: GIP; Body composition; Fat mass; Lean mass; Aging; Insulin resistance; Physical activity; GIP antagonism

Aging is associated with an increase in fat mass, thought to result from a sedentary lifestyle and *ad libitum* food intake over a prolonged period. Age-related accumulation of visceral fat is strongly associated with the development of insulin resistance [1–3]. On the other hand, reduction in skeletal muscle mass or sarcopenia also is a common feature of aging [4,5], increasing the risk for the development of insulin resistance [6]. To prevent the development of insulin resistance, various diet and exercise intervention trials have been conducted to favorably modify body composition by reducing fat mass while maintaining lean mass.

Gastric inhibitory polypeptide (GIP) is secreted from duodenal endocrine K cells in response to meal ingestion as an incretin, potentiating glucose-induced insulin secretion. Functional GIP receptors are expressed in adipose tissue [7] as well as in pancreatic β-cells, and GIP has been known to stimulate lipoprotein lipase activity and promote fatty acid incorporation into adipose tissue in the presence of insulin in cultured adipocytes [8–10]. Since GIP secretion is most strongly stimulated by fat ingestion [11,12], a high-fat diet is considered to be an ideal metabolic stress to induce hypersecretion of GIP for observation of

* Corresponding author. Address: Department of Internal Medicine, Division of Endocrinology, Diabetes and Geriatric Medicine, Akita University School of Medicine, Akita, Japan. Fax: +81 18 884 6117.
E-mail address: yamada@gipc.akita-u.ac.jp (Y. Yamada).
[1] Present address: Anjo Kosei Hospital, Japan.

0006-291X/$ - see front matter © 2007 Elsevier Inc. All rights reserved.
doi:10.1016/j.bbrc.2007.09.128

subsequent GIP action on adipocytes. The importance of GIP signaling on fat accumulation *in vivo* was first reported by Miyawaki et al. in mice with a targeted disruption of the GIP receptor gene (Gipr$^{-/-}$ mice), which exhibited reduced adiposity on a high-fat diet [9]. Since there was no difference in body weight between wild-type (WT) and Gipr$^{-/-}$ mice on a normal diet during a 50-week observation period [9], no attempt has been made to further investigate long-term GIP action in adipose tissue under normal nutritional conditions.

In the present study, we examined aging-associated changes in body composition using 10-week-old and 50-week-old WT and Gipr$^{-/-}$ mice on a normal diet. As in the previous study [9], the body weight of WT and Gipr$^{-/-}$ mice was almost identical, but computed tomography (CT) based-body composition analysis revealed that 50-week-old Gipr$^{-/-}$ mice had dramatically reduced fat mass and sustained lean mass compared with 50-week-old WT mice, which showed an age-related increase in fat mass and a decrease in lean mass.

Materials and methods

Animals. Generation of Gipr$^{-/-}$ mice was previously described [13]. Ten-week-old and 50-week-old male Gipr$^{-/-}$ mice and littermate WT controls on a C57BL/6 background were used. The animals had *ad libitum* access to standard rodent chow and water. Food intake (gram per mouse per day) was determined daily over 5 days in mice caged singly. All procedures were approved by the Animal Care Committee of Kyoto University Graduate School of Medicine.

CT-based body composition analysis. The mice were anesthetized with intraperitoneal injection of pentobarbital sodium (Dainippon Pharmaceutical, Japan) and their whole bodies were scanned along the body axis using the LaTheta (LCT-100M) experimental animal CT system (Aloka, Japan). Contiguous 1-mm slice images of the body including trunk and lower extremities were used for quantitative assessment using LaTheta software (version 1.00). Weights of total fat mass, which consists of visceral fat mass plus subcutaneous fat mass, and lean mass were determined and normalized by body weight.

Plasma hormone measurements. Plasma insulin, leptin, and adiponectin levels were determined by ELISA kits for mouse insulin (Shibayagi, Japan), mouse leptin (Morinaga, Japan), and mouse/rat adiponectin (Otsuka Pharmaceutical, Japan), respectively.

Insulin and glucose tolerance tests. For insulin tolerance test (ITT), 0.4 U/kg human insulin (Novonordisk, Denmark) was injected intraperitoneally after 5-h fasting. Oral glucose tolerance test (OGTT) was carried out following an overnight fast (16 h) and 2.0 g/kg glucose was loaded. Blood samples were taken at indicated times and blood glucose levels were measured by the enzyme-electrode method. HbA_{1c} was measured by immunoassay (DCA 2000 system, Bayer Diagnostics).

Insulin secretion from isolated islets. Isolation of pancreatic islets and batch incubation experiments were performed as described previously [14]. Briefly, 10 islets were collected in each tube and pre-incubated at 37 °C for 30 min in the medium containing 2.8 mM glucose, and incubated for another 30 min in the medium containing the indicated concentrations of glucose with 10^{-7} M human GIP or GLP-1 (Peptide Institute, Inc., Japan). Insulin secretion was measured by RIA using mouse insulin as a standard.

Telemetry recordings. Twelve- to 18-week-old WT and Gipr$^{-/-}$ mice weighing 27–30 g were used. The mice were anesthetized with pentobarbital sodium, and a small telemetric transmitter (TA10ETA-F20, Data Sciences Inc., USA) was implanted into the abdominal cavity. Seven to 14 days of recovery from the surgery was allowed before initiation of data collection. The mice were left undisturbed under a light/dark cycle of 14 h/10 h (lights on at 07:00 h and lights off at 21:00 h), and telemetry recordings for motor activity, body temperature (BT), and heart rate (HR) were performed every 2 min and averaged in 1-h bins using Dataquest A.R.T. software (version 2.1) (Data Sciences Inc.). The average for each bin from the same time point during a consecutive 5-day observation period was used for calculation.

Statistical analysis. Results are expressed as means ± SE. Statistical significance was assessed by ANOVA and unpaired Student's *t*-test, where appropriate. A P value of <0.05 was considered to be statistically significant.

Results

Aged Gipr$^{-/-}$ mice had reduced fat mass and sustained lean mass independent of changes in body weight or food intake

Body weight of WT and Gipr$^{-/-}$ mice was almost identical throughout the 50-week observation period (Fig. 1A). Body lengths measured at 10 and 50 weeks of age were also almost the same (data not shown). There was no difference in food intake between WT and Gipr$^{-/-}$ mice (Fig. 1B). CT-based analyses of body composition were performed as shown in Fig. 2A. There was no apparent difference in representative CT images showing abdominal fat (Fig. 2B, a) and thigh muscle (Fig. 2B, b) of 10-week-old WT and Gipr$^{-/-}$ mice. However, 50-week-old Gipr$^{-/-}$ mice had markedly less fat mass and a greater proportion of lean mass compared with 50-week-old WT mice (Fig. 2C). Total, subcutaneous, and visceral fat mass was similar in 10-week-old WT and Gipr$^{-/-}$ mice, but there

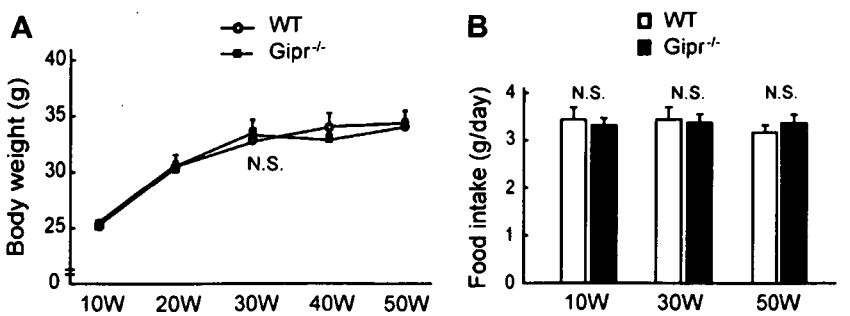

Fig. 1. Body weight and food intake. (A) Body weight of WT and Gipr$^{-/-}$ mice during the 50-week observation period. (B) Food intake (g/day) for each mouse was measured at 10, 30, and 50 weeks. n = 6–15 mice/group.

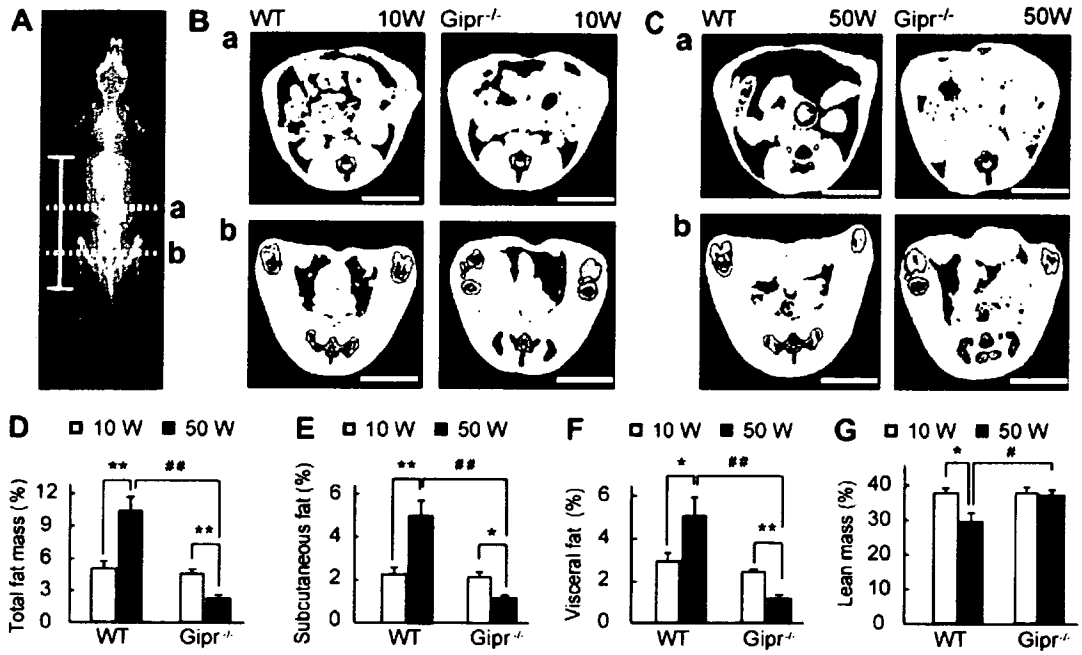

Fig. 2. CT-based body composition analyses. (A) The solid white bar indicates the observation area. Representative CT images showing abdominal fat (a) and thigh muscle (b) of 10-week-old (B) and 50-week-old (C) WT and Gipr$^{-/-}$ mice. The pink, yellow, and light blue areas represent visceral fat, subcutaneous fat, and lean mass, respectively. (D) Total fat mass, (E) subcutaneous fat mass, (F) visceral fat mass, and (G) lean mass, normalized to body weight, in 10-week-old and 50-week-old WT and Gipr$^{-/-}$ mice. $n = 6$–8 mice/group. $^{*}P < 0.05$; $^{**}P < 0.01$, 10-week-old vs 50-week-old mice, $^{\#}P < 0.05$; $^{\#\#}P < 0.01$, WT vs Gipr$^{-/-}$ mice. Scale bars, 1 cm. (For interpretation of the references to color in this figure legend, the reader is referred to the web version of this article.)

was a considerable difference in fat mass between 50-week-old WT and Gipr$^{-/-}$ mice (Fig. 2D–F). On the other hand, the weight of lean body mass was significantly increased in 50-week-old Gipr$^{-/-}$ mice (weights of lean body mass: 9.6 ± 0.5, 9.7 ± 0.6, 10.1 ± 0.7, and 12.4 ± 0.5 g for 10-week-old WT, 10-week-old Gipr$^{-/-}$, 50-week-old WT, and 50-week-old Gipr$^{-/-}$ mice, respectively, $P < 0.05$, 50-week-old WT vs Gipr$^{-/-}$ mice, $P < 0.01$, 10-week-old vs 50-week-old Gipr$^{-/-}$ mice). When normalized by body weight, lean mass was significantly decreased in 50-week-old WT mice, while 50-week-old Gipr$^{-/-}$ mice maintained the same percentage of lean mass as the young mice (Fig. 2G). There was no difference in organ weight between 50-week-old WT and Gipr$^{-/-}$ mice (liver weight: WT 1.64 ± 0.12 g vs Gipr$^{-/-}$ 1.63 ± 0.10 g, intestinal weight: WT 3.69 ± 0.21 g vs Gipr$^{-/-}$ 3.53 ± 0.40 g) as well as in 10-week-old WT and Gipr$^{-/-}$ mice (data not shown).

Aged Gipr$^{-/-}$ mice showed improved insulin sensitivity and amelioration in glucose tolerance

Insulin sensitivity was evaluated by ITT, and the glucose-lowering effect of insulin was decreased in 50-week-old WT mice compared with 10-week-old WT mice, indicating that WT mice had developed age-related insulin resistance (Fig. 3A). To the contrary, 50-week-old Gipr$^{-/-}$ mice were more insulin sensitive than 10-week-old Gipr$^{-/-}$ mice (Fig. 3B). There was no difference in glucose tolerance between 10-week-old and 50-week-old WT mice (Fig. 3C), but in 50-week-old WT mice, a compensatory increase in insulin secretion was required to achieve the same blood glucose levels as those in 10-week-old WT mice (Fig. 3E). In 50-week-old Gipr$^{-/-}$ mice, fasting and 15-min glucose levels were significantly decreased compared with 10-week-old Gipr$^{-/-}$ mice (76.4 ± 4.6 vs 56.0 ± 9.1 mg/dl at 0 min, $P < 0.01$, and 386.8 ± 20.6 vs 349.7 ± 46.0 mg/dl at 15 min, $P < 0.05$, for 10-week-old vs 50-week-old Gipr$^{-/-}$ mice, respectively), and the glycemic excursion between 30 min and 120 min was lower than that of 10-week-old Gipr$^{-/-}$ mice (Fig. 3D), although plasma insulin levels were not increased (Fig. 3F). Although Gipr$^{-/-}$ mice exhibited elevated post-challenge blood glucose levels, overall glycemic control as shown by HbA_{1c} was not worse in Gipr$^{-/-}$ mice compared with that in WT mice (3.10 ± 0.16, 2.84 ± 0.12, 2.80 ± 0.11, and $2.65 \pm 0.1\%$ for 10-week-old WT, 10-week-old Gipr$^{-/-}$, 50-week-old WT, and 50-week-old Gipr$^{-/-}$ mice, respectively). We also determined insulin secretion from isolated islets and found that the insulin secretory response to glucose and GLP-1 stimulation was intact in 10-week-old and 50-week-old Gipr$^{-/-}$ mice compared with their WT controls (Fig. S1(A) and S1(B)).

Aged Gipr$^{-/-}$ mice showed favorable changes in plasma adipocytokine levels and spontaneous hyperactivity

Consistent with fat mass, plasma leptin levels were significantly lower in 50-week-old Gipr$^{-/-}$ mice than in

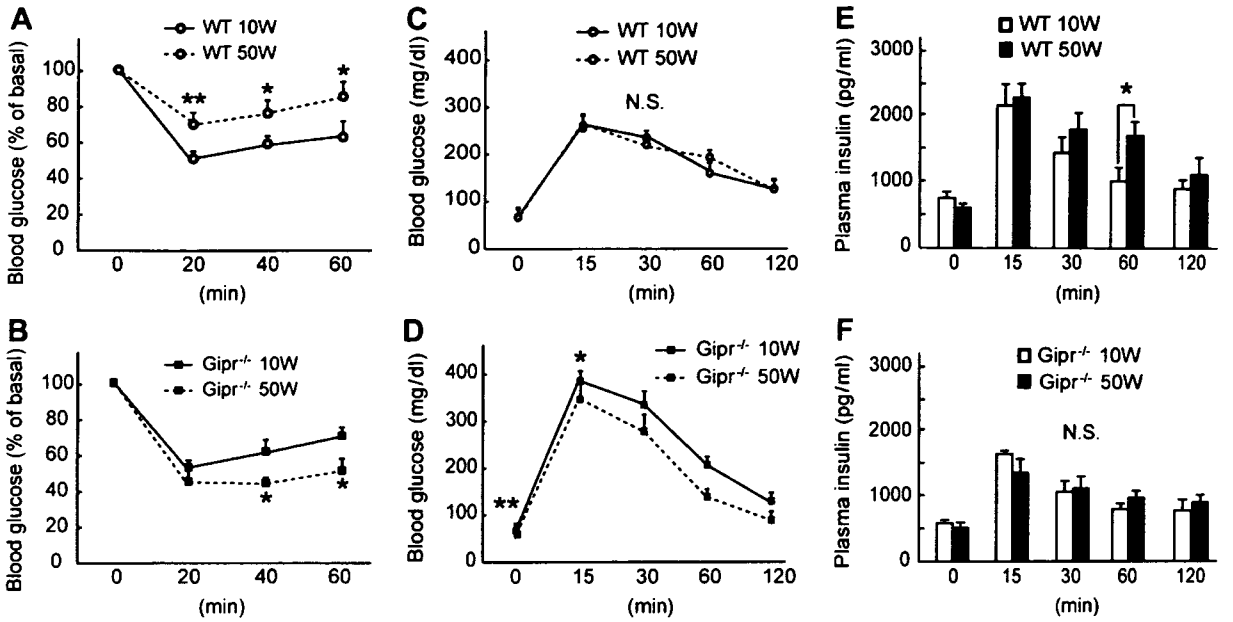

Fig. 3. Insulin and glucose tolerance tests. Results of insulin tolerance tests in 10-week-old and 50-week-old WT (A) and Gipr$^{-/-}$ (B) mice. $n = 6$–10 mice/group. Blood glucose levels during oral glucose tolerance test (OGTT) in 10-week-old and 50-week-old WT mice (C) and 10-week-old and 50-week-old Gipr$^{-/-}$ mice (D). Plasma insulin levels during OGTT (B) in 10-week-old and 50-week-old WT mice (E) and 10-week-old and 50-week-old Gipr$^{-/-}$ mice (F). $n = 5$–8 mice/group. $^{*}P < 0.05$; $^{**}P < 0.01$, 10-week-old vs 50-week-old mice.

50-week-old WT mice (Fig. 4A). On the other hand, plasma adiponectin levels were significantly higher in 50-week-old Gipr$^{-/-}$ mice than in 50-week-old WT mice (Fig. 4B). To investigate the underlying mechanism of increased lean mass, we used implanted telemetry chips to measure the 24-h profile of physical activity. WT and Gipr$^{-/-}$ mice both exhibited a robust rhythm of physical activity with intense activity during the dark phase and rest during the light phase (Fig. 4C). The average activity counts during a consecutive 5-day observation period showed that spontaneous activity was significantly increased in Gipr$^{-/-}$ mice both in light and dark phases

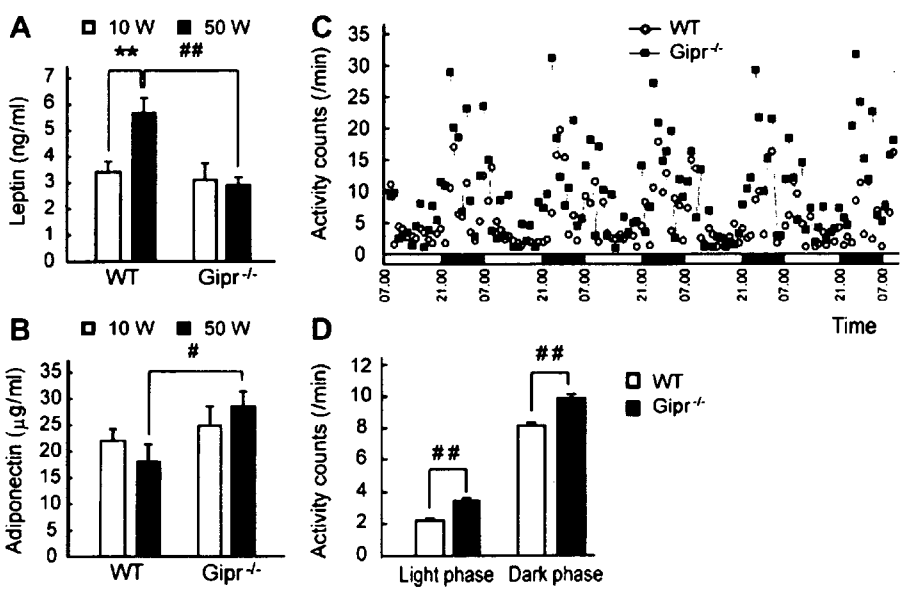

Fig. 4. Plasma adipocytokine levels and physical activity. (A) Plasma leptin and (B) adiponectin levels in 10-week-old and 50-week-old WT and Gipr$^{-/-}$ mice. $n = 6$–10 mice/group. (C) Representative circadian patterns of physical activity in a WT and Gipr$^{-/-}$ mouse under a 14 h/10 h light/dark cycle during a consecutive 5-day observation period. The white and black bar below the figure represents light phase and dark phase, respectively. (D) Average activity counts per minute in WT and Gipr$^{-/-}$ mice. $n = 5$ mice/group. $^{**}P < 0.01$, 10-week-old vs 50-week-old mice, $^{\#}P < 0.05$; $^{\#\#}P < 0.01$, WT vs Gipr$^{-/-}$ mice.

(Fig. 4D). However, BT in dark phase (Fig. S1(C) and S1(D)) and HR in both light and dark phases (Fig. S1(E) and S1(F)), measured simultaneously, were paradoxically decreased in Gipr$^{-/-}$ mice compared with WT mice despite increased physical activity.

Discussion

GIP was originally designated gastric inhibitory polypeptide for its influence on gastric acid secretion, and was later designated glucose-dependent insulinotropic polypeptide for its stimulation of insulin secretion from pancreatic β-cells. Studies using Gipr$^{-/-}$ mice have shown that GIP also has physiological roles in fat accumulation into adipose tissues [9] and calcium accumulation into bone [15], and thus a more appropriate referent of the acronym, gut-derived nutrient-intake polypeptide, has been recently proposed to more accurately reflect its physiological function [16]. The importance of inhibition of GIP signaling on fat accumulation *in vivo* was first demonstrated by Miyawaki et al., who found that male Gipr$^{-/-}$ mice fed a high-fat diet exhibit dramatically lesser adiposity than WT mice [9]. In addition, Hansotia et al. showed that single incretin (either GIP or glucagon-like peptide-1, GLP-1) receptor knockout mice as well as double incretin (both GIP and GLP-1) receptor knockout mice exhibited reduced body weight gain and adipose tissue accretion after a 20-week high-fat diet [17].

In the present study, we clearly show that 50-week-old Gipr$^{-/-}$ mice on a normal diet had reduced fat mass but sustained lean mass independent of changes in body weight or food intake, while 50-week-old WT mice showed dramatically increased fat mass and decreased lean mass, a characteristic of aging-associated changes in body composition. In young mice on normal diet, Xie et al. reported that the percentage of total fat was significantly increased and the amount of lean mass was reduced in 1-month-old and 5-month-old Gipr$^{-/-}$ females [18], however their results and our results are incommensurable because of the differences in sex, age, and breeding environments.

We also demonstrated that such alterations in body composition protected Gipr$^{-/-}$ mice from the development of insulin resistance (Fig. 3B). In C57BL/6 mice on a normal diet, glucose tolerance itself does not necessarily deteriorate with age because glucose-stimulated insulin secretion increases to compensate for age-related insulin resistance [19]. In our study, aged WT mice retained normal glucose tolerance, although a compensatory increase in insulin secretion was required to achieve the same blood glucose levels as in young mice. On the other hand, aged Gipr$^{-/-}$ mice showed better glucose tolerance during OGTT than in young Gipr$^{-/-}$ mice without incremental insulin secretion. Although Gipr$^{-/-}$ mice showed mild hyperglycemia compared with WT mice at early phases after oral glucose challenge, overall glycemic control as shown by HbA_{1c} was not worse in Gipr$^{-/-}$ mice. Moreover, the insulin secretory response to glucose and GLP-1 stimulation was intact in the islets of Gipr$^{-/-}$ mice compared with those of WT controls, indicating that β-cell function was not impaired by long-term inhibition of GIP signaling. We therefore conclude that aged Gipr$^{-/-}$ mice are protected from the development of aging-associated insulin resistance, which is associated with amelioration in glucose tolerance.

Stability of lean mass is another most important anti-aging phenomenon observed in aged Gipr$^{-/-}$ mice. Skeletal muscle accounts for more than half (~55%) of total lean mass, and maintenance of skeletal muscle mass is important for its metabolic quality as well as physical strength and functional status. There is an ongoing reduction of skeletal muscle mass in weight-stable elderly men and women [4,5], suggesting that weight stability in older individuals does not imply body composition stability, however, Gipr$^{-/-}$ mice gained lean mass with age, maintaining the same percentage of lean mass as the young mice (Fig. 2G). Favorable body composition with decreased fat mass and sustained lean mass can be promoted by physical exercise [20]. Our results clearly show that Gipr$^{-/-}$ mice are spontaneously hyperactive (Fig. 3C and D), which may contribute to favorable body composition and improved insulin sensitivity in older age. Surprisingly, BT and HR measured simultaneously were decreased in Gipr$^{-/-}$ mice compared with WT mice despite increased physical activity, characteristics resembling the physiological changes that take place in long-lived calorie restricted animals [21–23].

In conclusion, we have demonstrated that long-term inhibition of GIP signaling prevents development of aging-associated insulin resistance through body composition changes. Considering the difficulty of maintaining dietary restriction and exercise training for a prolonged period, GIP antagonism might be considered for further investigation as a therapeutic option against metabolic disorders related to aging.

Acknowledgments

This study was supported in part by Grants-in-Aid for Scientific Research from the Ministry of Education, Culture, Sports, Science and Technology, Japan, and by Health and Labour Sciences Research Grants from the Ministry of Health, Labour and Welfare, Japan.

Appendix A. Supplementary data

Supplementary data associated with this article can be found, in the online version, at doi:10.1016/j.bbrc.2007.09.128.

References

[1] P.J. Coon, E.M. Rogus, D. Drinkwater, D.C. Muller, A.P. Goldberg, Role of body fat distribution in the decline in insulin sensitivity and

glucose tolerance with age, J. Clin. Endocrinol. Metab. 75 (1992) 1125–1132.
[2] W.M. Kohrt, J.P. Kirwan, M.A. Staten, R.E. Bourey, D.S. King, J.O. Holloszy, Insulin resistance in aging is related to abdominal obesity, Diabetes 42 (1993) 273–281.
[3] S.B. Racette, E.M. Evans, E.P. Weiss, J.M. Hagberg, J.O. Holloszy, Abdominal adiposity is a stronger predictor of insulin resistance than fitness among 50–95 year olds, Diabetes Care 29 (2006) 673–678.
[4] D. Gallagher, E. Ruts, M. Visser, S. Heshka, R.N. Baumgartner, J. Wang, R.N. Pierson, F.X. Pi-Sunyer, S.B. Heymsfield, Weight stability masks sarcopenia in elderly men and women, Am. J. Physiol. Endocrinol. Metab. 279 (2000) E366–E375.
[5] V.A. Hughes, W.R. Frontera, R. Roubenoff, W.J. Evans, M.A. Singh, Longitudinal changes in body composition in older men and women: role of body weight change and physical activity, Am. J. Clin. Nutr. 76 (2002) 473–481.
[6] A.S. Ryan, Insulin resistance with aging: effects of diet and exercise, Sports Med. 30 (2000) 327–346.
[7] R.G. Yip, M.O. Boylan, T.J. Kieffer, M.M. Wolfe, Functional GIP receptors are present on adipocytes, Endocrinology 139 (1998) 4004–4007.
[8] B. Beck, J.P. Max, Gastric inhibitory polypeptide enhancement of the insulin effect on fatty acid incorporation into adipose tissue in the rat, Regul. Pept. 7 (1983) 3–8.
[9] K. Miyawaki, Y. Yamada, N. Ban, Y. Ihara, K. Tsukiyama, H. Zhou, S. Fujimoto, A. Oku, K. Tsuda, S. Toyokuni, H. Hiai, W. Mizunoya, T. Fushiki, J.J. Holst, M. Makino, A. Tashita, Y. Kobara, Y. Tsubamoto, T. Jinnouchi, T. Jomori, Y. Seino, Inhibition of gastric inhibitory polypeptide signaling prevents obesity, Nat. Med. 8 (2002) 738–742.
[10] S.J. Kim, C. Nian, C.H. McIntosh, Activation of lipoprotein lipase by glucose-dependent insulinotropic polypeptide in adipocytes. A role for a protein kinase B, LKB1, and AMP-activated protein kinase cascade, J. Biol. Chem. 282 (2007) 8557–8567.
[11] J.M. Falko, S.E. Crockett, S. Cataland, E.L. Mazzaferri, Gastric inhibitory polypeptide (GIP) stimulated by fat ingestion in man, J. Clin. Endocrinol. Metab. 41 (1975) 260–265.
[12] T. Krarup, J.J. Holst, K.L. Larsen, Responses and molecular heterogeneity of IR-GIP after intraduodenal glucose and fat, Am. J. Physiol. 249 (1985) E195–E200.
[13] K. Miyawaki, Y. Yamada, H. Yano, H. Niwa, N. Ban, Y. Ihara, A. Kubota, S. Fujimoto, M. Kajikawa, A. Kuroe, K. Tsuda, H. Hashimoto, T. Yamashita, T. Jomori, F. Tashiro, J. Miyazaki, Y. Seino, Glucose intolerance caused by a defect in the entero-insular axis: a study in gastric inhibitory polypeptide receptor knockout mice, Proc. Natl. Acad. Sci. USA 96 (1999) 14843–14847.
[14] C. Yamada, K. Nagashima, A. Takahashi, H. Ueno, Y. Kawasaki, Y. Yamada, Y. Seino, N. Inagaki, Gatifloxacin acutely stimulates insulin secretion and chronically suppresses insulin biosynthesis, Eur. J. Pharmacol. 553 (2006) 67–72.
[15] K. Tsukiyama, Y. Yamada, C. Yamada, N. Harada, Y. Kawasaki, M. Ogura, K. Bessho, M. Li, N. Amizuka, M. Sato, N. Udagawa, N. Takahashi, K. Tanaka, Y. Oiso, Y. Seino, Gastric inhibitory polypeptide as an endogenous factor promoting new bone formation after food ingestion, Mol. Endocrinol. 20 (2006) 1644–1651.
[16] Y. Yamada, K. Miyawaki, K. Tsukiyama, N. Harada, C. Yamada, Y. Seino, Pancreatic and extrapancreatic effects of gastric inhibitory polypeptide, Diabetes 55 (2006) S86–S91.
[17] T. Hansotia, A. Maida, G. Flock, Y. Yamada, K. Tsukiyama, Y. Seino, D.J. Drucker, Extrapancreatic incretin receptors modulate glucose homeostasis, body weight, and energy expenditure, J. Clin. Invest. 117 (2007) 143–152.
[18] D. Xie, H. Cheng, M. Hamrick, Q. Zhong, K.H. Ding, D. Correa, S. Williams, A. Mulloy, W. Bollag, R.J. Bollag, R.R. Runner, J.C. McPherson, K. Insogna, C.M. Isales, Glucose-dependent insulinotropic polypeptide receptor knockout mice have altered bone turnover, Bone 37 (2005) 759–769.
[19] E.H. Leiter, F. Premdas, D.E. Harrison, L.G. Lipson, Aging and glucose homeostasis in C57BL/6J male mice, FASEB J. 2 (1988) 2807–2811.
[20] P. Stiegler, A. Cunliffe, The role of diet and exercise for the maintenance of fat-free mass and resting metabolic rate during weight loss, Sports Med. 36 (2006) 239–262.
[21] L.K. Heilbronn, E. Ravussin, Calorie restriction and aging: review of the literature and implications for studies in humans, Am. J. Clin. Nutr. 78 (2003) 361–369.
[22] D. Chen, A.D. Steele, S. Lindquist, L. Guarente, Increase in activity during calorie restriction requires Sirt1, Science 310 (2005) 1641.
[23] M.P. Mattson, R. Wan, Beneficial effects of intermittent fasting and caloric restriction on the cardiovascular and cerebrovascular systems, J. Nutr. Biochem. 16 (2005) 129–137.

Cell Metabolism

Central Melanocortin Signaling Restores Skeletal Muscle AMP-Activated Protein Kinase Phosphorylation in Mice Fed a High-Fat Diet

Tomohiro Tanaka,[1] Hiroaki Masuzaki,[1,*] Shintaro Yasue,[1] Ken Ebihara,[1] Tetsuya Shiuchi,[2] Takako Ishii,[1] Naoki Arai,[1] Masakazu Hirata,[1] Hiroshi Yamamoto,[3] Tatsuya Hayashi,[4] Kiminori Hosoda,[1] Yasuhiko Minokoshi,[2] and Kazuwa Nakao[1]

[1] Department of Medicine and Clinical Science, Kyoto University Graduate School of Medicine, Kyoto 606-8507, Japan
[2] Department of Developmental Physiology, National Institute for Physiological Sciences, Okazaki 444-8585, Japan
[3] Department of Surgery, Shiga University of Medical Science, Otsu 520-2192, Japan
[4] Department of Human Coexistence, Kyoto University Graduate School of Human and Environmental Studies, Kyoto 606-8501, Japan
*Correspondence: hiroaki@kuhp.kyoto-u.ac.jp
DOI 10.1016/j.cmet.2007.04.004

SUMMARY

Little is known about the role of the central melanocortin system in the control of fuel metabolism in peripheral tissues. Skeletal muscle AMP-activated protein kinase (AMPK) is activated by leptin and serves as a master regulator of fatty acid β-oxidation. To elucidate an unidentified role of the central melanocortin system in muscle AMPK regulation, we treated conscious, unrestrained mice intracerebroventricularly with the melanocortin agonist MT-II or the antagonist SHU9119. MT-II augmented phosphorylation of AMPK and its target acetyl-CoA carboxylase (ACC) independent of caloric intake. Conversely, AMPK/ACC phosphorylation by leptin was abrogated by the coadministration of SHU9119 or in KKA^{y} mice, which centrally express endogenous melanocortin antagonist. Importantly, high-fat-diet-induced attenuation of AMPK/ACC phosphorylation in leptin-overexpressing transgenic mice was not reversed by central leptin but was markedly restored by MT-II. Our data provide evidence for the critical role of the central melanocortin system in the leptin-skeletal muscle AMPK axis and highlight the system as a therapeutic target in leptin resistance.

INTRODUCTION

Leptin augments fatty acid β-oxidation in skeletal muscle and enhances whole-body insulin sensitivity, thereby serving as a promising therapeutic candidate for the treatment of insulin resistance and dyslipidemia (Shimabukuro et al., 1997; Minokoshi et al., 2002). In agreement with this notion, we and others have demonstrated the clinical efficacy of leptin in the treatment of diabetes, dyslipidemia, and steatosis in patients with lipodystrophy (Oral et al., 2002; Ebihara et al., 2007). The clinical application of leptin has been hampered, however, by the fact that leptin does not fully exert its metabolic effect in prevalent forms of human obesity (Maffei et al., 1995) and in diet-induced obese rodents (El-Haschimi et al., 2000).

Using transgenic skinny mice overexpressing leptin in liver (LepTg mice), we recently demonstrated that enhanced lipid metabolism and insulin sensitivity in LepTg mice are attenuated on a high-fat diet (HFD) (HFD-LepTg) despite persistent hyperleptinemia, compared with HFD-fed nontransgenic (HFD-non-Tg) littermates (Tanaka et al., 2005). Even with pronounced hyperleptinemia, skeletal muscle AMPK activity is attenuated in HFD-LepTg mice to the level of HFD-non-Tg mice (Tanaka et al., 2005). Noteworthy is the fact that switching HFD back to a standard diet (STD) leads to a significant recovery of muscle AMPK activity in LepTg mice before they regain their skinny phenotype (Tanaka et al., 2005), suggesting the reversible nature of the dietary lipid-induced leptin resistance.

AMPK is activated by decreased energy stores and orchestrates energy-sparing reactions in a cell-specific manner (Hardie et al., 2006). In skeletal muscle cells, AMPK activation stimulates glucose uptake, glycolysis, fatty acid β-oxidation, and mitochondrial biogenesis (Hardie et al., 2006) and critically mediates leptin-induced fatty acid β-oxidation (Minokoshi et al., 2002). Our previous work demonstrated that skeletal muscle AMPK activity closely parallels insulin sensitivity and inversely correlates with energy efficiency in LepTg mice under STD or HFD feeding (Tanaka et al., 2005), indicating that AMPK activity should be a novel biochemical marker of leptin sensitivity in vivo.

The central melanocortin system consists of endogenous melanocortin agonists and receptors. Endogenous agonist is synthesized as pro-opiomelanocortin (POMC) preprohormone and is proteolytically cleaved to produce melanocyte-stimulating hormones (MSHs). In the brain,

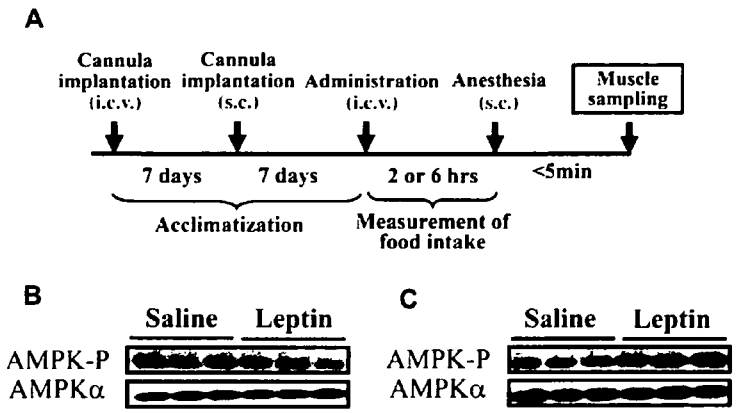

Figure 1. Establishment of the Experimental Protocol

(A) After intracerebroventricular (i.c.v.) and subcutaneous (s.c.) cannula implantation, mice were acclimatized and trained for handling. On the day of sampling, agents were administered i.c.v. in free-moving nonanesthetized mice. Food intake was measured and anesthesia was introduced s.c.

(B) Representative blots for phospho-AMPK and AMPKα in soleus muscle after leptin (0.5 μg) i.c.v. under intraperitoneal (i.p.) anesthesia. Muscles were sampled after another i.p. injection of the anesthetic agent.

(C) Representative blots for phospho-AMPK and AMPKα using the protocol in (A).

POMC is principally expressed in the arcuate nucleus of the hypothalamus (ARC) and the nucleus of the solitary tract (NTS) of the brainstem (Schwartz et al., 1997). The majority of POMC-expressing neurons in the ARC coexpress functional leptin receptor and mediate the anorectic effect of leptin (Cowley et al., 2001; Seeley et al., 1997). Although mouse models and human subjects with defective melanocortin signaling develop obesity (Huszar et al., 1997; Fan et al., 1997; Kobayashi et al., 2002; Farooqi et al., 2003), it remains largely unknown whether the central melanocortin system regulates fuel metabolism in skeletal muscle. In this context, we demonstrate here that the central melanocortin system is a critical mediator of leptin-induced skeletal muscle AMPK activation. In sharp contrast to leptin, melanocortin agonist retains its AMPK-activating potency even in mice fed a HFD.

RESULTS

Assessment of Skeletal Muscle AMPK Phosphorylation after Intracerebroventricular Administration in Conscious, Unrestrained Mice

AMPK activity is readily altered by various stimuli such as muscle contraction and ischemia (Hardie et al., 2006). To obtain reproducible results, establishment of an elaborately organized protocol was indispensable to minimize nonspecific AMPK activation. Intracerebroventricular (i.c.v.) and subcutaneous (s.c.) cannulae were implanted 14 and 7 days prior to the experiment, respectively, so that body weight recovered to the level of nonoperated mice on the sampling day (data not shown). Subcutaneous instead of intravenous cannulation was used to avoid a major weight loss. Agents were injected i.c.v. in well-acclimatized, nonanesthetized, free-moving mice. Anesthesia was introduced gently through s.c. cannula, and samples were obtained within 5 min (Figure 1A).

We first administered leptin i.c.v. under intraperitoneal (i.p.) anesthesia and sampled muscle after another i.p. injection of the anesthetic agent. By this method, we could not see a reproducible increase in phospho-AMPK levels by leptin (Figure 1B). In contrast, by the protocol in Figure 1A, leptin-induced increase in AMPK phosphorylation was clear (Figure 1C). In addition, we could also measure food intake, which was unaffected by anesthesia or by the nervousness of the mouse, precisely.

Melanocortin Agonist Increases AMPK Phosphorylation in Skeletal Muscle

Melanotan II (MT-II) is a potent melanocortin 3/4 receptor (MC3R/4R) agonist (Fan et al., 1997). Although it is known that central treatment with MT-II reduces food intake (Fan et al., 1997), its effect on skeletal muscle fuel metabolism has not been thoroughly addressed. We treated 8-week-old male C57BL/6 mice with leptin (0.5 μg) or MT-II (3.5 μg) i.c.v. and sampled the soleus muscle 6 hr later. Leptin i.c.v. significantly increased AMPK phosphorylation in the soleus muscle (Figure 2A). Likewise, MT-II i.c.v. increased phospho-AMPK levels by 69% ± 19% ($p < 0.05$ versus vehicle, $n = 7$). Neither leptin nor MT-II altered AMPKα protein levels, resulting in a 78% ± 14% ($p < 0.05$ versus vehicle, $n = 7$) and 64% ± 20% ($p < 0.05$ versus vehicle, $n = 7$) increase in phospho-AMPK/AMPKα ratio by leptin and MT-II, respectively (Figure 2A).

ACC is an established target of AMPK in muscle (Hardie et al., 2006). Phosphorylation of ACC by AMPK inhibits ACC enzyme activity and reduces the production of malonyl-CoA, thereby activating fatty acid β-oxidation (Minokoshi et al., 2002). In the present study, ACC phosphorylation was also augmented by MT-II by 90% ± 28% ($p < 0.05$ versus vehicle, $n = 7$) an increase comparable to that by leptin (83% ± 12%) ($p < 0.05$ versus vehicle, $n = 7$) (Figure 2B). Neither leptin nor MT-II i.c.v. altered ACC protein levels (see Figure S1A in the Supplemental Data available with this article online).

LepTg mice exhibit a more than 10-fold increase in plasma leptin levels, a paucity of adipose tissue, and enhanced glucose and lipid metabolism (Ogawa et al., 1999). In LepTg mice, soleus muscle AMPK phosphorylation and ACC phosphorylation were substantially increased compared with wild-type littermates (insets in Figures 2A and 2B). The levels of AMPK and ACC phosphorylation in MT-II or leptin i.c.v.-treated mice were comparable to those in LepTg mice.

AMPK phosphorylation was increased 2 hr after leptin i.c.v. by 63% ± 11% ($p < 0.05$ versus vehicle, $n = 7$) and maintained this level up to 6 hr (75% ± 10% increase)

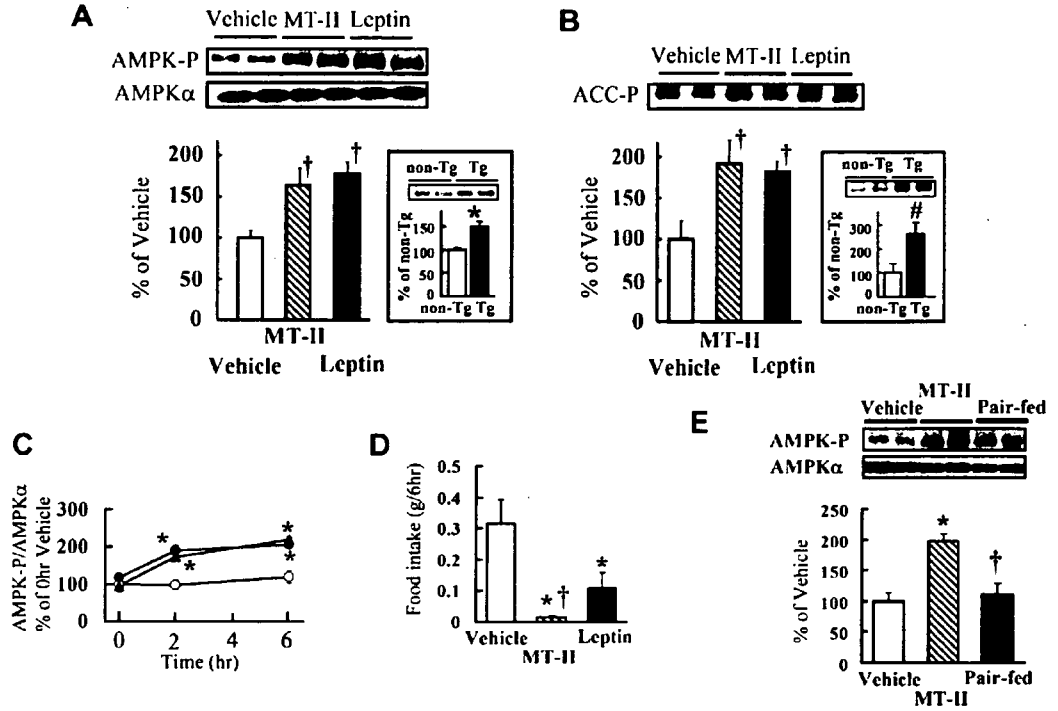

Figure 2. Increased Skeletal Muscle AMPK and ACC Phosphorylation after Intracerebroventricular MT-II Treatment

(A) Representative blots for phospho-AMPK and AMPKα in soleus muscle sampled 6 hr after MT-II (3.5 μg) or leptin (0.5 μg) i.c.v. The graph shows quantification of phospho-AMPK divided by that of AMPKα (phospho-AMPK/AMPKα ratio). †$p < 0.05$ versus vehicle, n = 7. Inset: Blots for phospho-AMPK and phospho-AMPK/AMPKα in LepTg mice. *$p < 0.05$ versus non-Tg, n = 6. In this and all other figures, error bars represent ± SEM.

(B) Representative blots for phospho-ACC in soleus muscle 6 hr after MT-II or leptin i.c.v. †$p < 0.05$ versus vehicle, n = 7. The graph shows the quantified data. Inset: Phospho-ACC in LepTg. #$p < 0.05$ versus non-Tg, n = 6.

(C) Phospho-AMPK/AMPKα before and 2 and 6 hr after MT-II or leptin i.c.v. ○, vehicle; ●, leptin; ▲, MT-II; *$p < 0.05$ versus vehicle, n = 6.

(D) Cumulative food intake over 6 hr. *$p < 0.05$ versus vehicle, †$p < 0.05$ versus leptin, n = 7.

(E) Blots for phospho-AMPK and AMPKα, and graph showing phospho-AMPK/AMPKα in MT-II-treated mice and vehicle-treated mice pair-fed with MT-II-treated counterparts. *$p < 0.05$ versus vehicle, †$p < 0.05$ versus MT-II, n = 6.

($p < 0.05$ versus vehicle, n = 7) (Figure 2C). Likewise, MT-II i.c.v. led to a significant increase in AMPK phosphorylation over 2 hr, by 100% ± 7% ($p < 0.05$ versus vehicle, n = 7), and this level was maintained until the 6 hr point (125% ± 12% increase) ($p < 0.05$ versus vehicle, n = 7) (Figure 2C). To determine whether increased AMPK phosphorylation is paralleled by any change in plasma glucose or insulin levels, mice were fasted for 3 hr, MT-II was injected i.c.v., and blood samples were obtained 6 hr later. No difference was observed in plasma glucose (vehicle 122 ± 12 mg/dl versus MT-II 125 ± 9 mg/dl; not significant [NS], n = 6) or insulin (vehicle 1.84 ± 0.10 ng/ml versus MT-II 1.77 ± 0.08 ng/ml; NS, n = 6) levels between vehicle- and MT-II-treated mice.

Leptin or MT-II i.c.v. suppressed food intake (Figure 2D). Over 6 hr, mice treated with leptin i.c.v. consumed 0.11 ± 0.05 g of food ($p < 0.05$ versus vehicle), while vehicle-treated mice consumed 0.32 ± 0.08 g. Mice treated with MT-II i.c.v. consumed 0.02 g with a standard deviation of less than 0.01 g ($p < 0.05$ versus vehicle, $p < 0.05$ versus leptin, n = 7). To rule out possible involvement of the anorectic effect of MT-II in increased AMPK phosphorylation in the muscle, we pair-fed vehicle-treated mice with mice treated with MT-II. In contrast to MT-II-treated mice, AMPK phosphorylation was not altered in the pair-fed mice ($p < 0.05$ versus vehicle, n = 6) (Figure 2E), showing that MT-II-induced AMPK phosphorylation is independent of suppression of food intake.

We next examined whether peripheral MT-II administration has a similar effect on skeletal muscle AMPK. We administered a single dose of MT-II (10 μg, s.c.) and examined AMPK and ACC phosphorylation 6 hr later. Peripheral treatment with MT-II at this dose also significantly increased AMPK (61% ± 19%) and ACC (69% ± 20%) phosphorylation compared with vehicle ($p < 0.05$ versus vehicle, n = 5) (data not shown).

Leptin-Induced AMPK and ACC Phosphorylation Is Attenuated by Melanocortin Antagonism

Leptin activates the hypothalamic melanocortin pathway (Schwartz et al., 1997; Cowley et al., 2001) and enhances skeletal muscle AMPK activity (Minokoshi et al., 2002). To test whether the central melanocortin system is involved in leptin-induced AMPK activation in the muscle, we injected

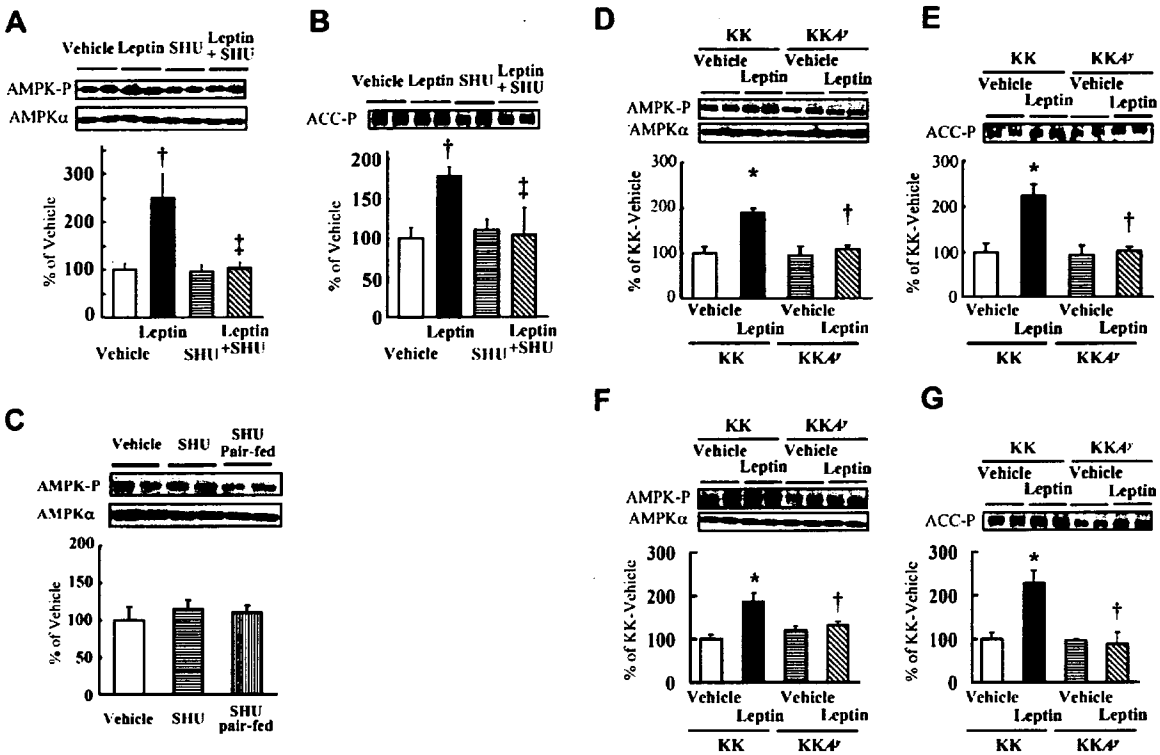

Figure 3. Attenuation of Leptin-Induced Muscle AMPK and ACC Phosphorylation by Pharmacologic or Genetic Melanocortin Blockade

(A, C, D, and F) Blots for phospho-AMPK and AMPKα, and graph showing phospho-AMPK/AMPKα.

(B, E, and G) Blots for phospho-ACC and quantified data.

Coadministration of SHU9119 (1.0 μg) i.c.v. attenuated leptin (0.5 μg)-induced increase in AMPK (A) and ACC (B) phosphorylation (†$p < 0.05$ versus vehicle, ‡$p < 0.05$ versus leptin, $n = 7$). Phospho-AMPK/AMPKα was not affected in mice treated with SHU9119 alone or in SHU9119-treated mice pair-fed with vehicle-treated mice (A and C). Leptin i.c.v. significantly increased AMPK (D and F) and ACC phosphorylation (E and G) in KK mice, while the increase was attenuated in both 6-week-old (D and E) and 10-week-old KKA^y mice (F and G) (*$p < 0.05$ versus KK-vehicle, †$p < 0.05$ versus KK-leptin, $n = 6$; data are % of KK-vehicle).

SHU9119, a MC3R/4R antagonist (Fan et al., 1997). Coadministration of SHU9119 i.c.v. (1.0 μg) suppressed leptin-induced increase in AMPK (Figure 3A) and ACC phosphorylation (Figure 3B) to the vehicle level (phospho-AMPK/AMPKα 150% ± 49% increase by leptin versus 4% ± 10% increase by leptin + SHU9119; phospho-ACC 79% ± 13% increase by leptin versus 6% ± 34% increase by leptin + SHU9119; $p < 0.05$, $n = 7$). Intracerebroventricular injection of SHU9119 alone did not affect AMPK (5% ± 9% decrease) or ACC (10% ± 12% increase) phosphorylation (Figures 3A and 3B). Central administration of SHU9119 alone or in conjunction with leptin did not change ACC protein levels (Figure S1B). SHU9119 i.c.v. significantly increased food intake over the following 6 hr (vehicle 0.35 ± 0.08 g versus SHU9119 0.49 ± 0.09 g; $p < 0.05$, $n = 6$). To test the hypothesis that increased food intake caused by SHU9119 may play a role in skeletal muscle AMPK regulation, we compared AMPK/ACC phosphorylation in vehicle-treated mice, SHU9119-treated mice, and SHU9119-treated mice pair-fed with vehicle-treated mice. Neither treatment with SHU9119 only nor treatment with SHU9119 plus pair-feeding had any effect on AMPK (SHU9119 15% ± 12% increase, SHU9119 plus pair-feeding 10% ± 10% increase versus vehicle) (Figure 3C) or ACC phosphorylation (SHU9119 8% ± 10% decrease, SHU9119 plus pair-feeding 13% ± 5% versus vehicle; NS, $n = 6$) (data not shown).

KKA^y mice (A^y mutants on a KK background) ectopically express agouti protein, an endogenous melanocortin receptor antagonist, throughout the body, including in the hypothalamus, and exhibit progressive obesity in addition to yellow coat color (Lu et al., 1994). Here we used preobese (6 weeks old, KK 29.0 ± 0.8 g versus KKA^y 29.1 ± 1.0 g; NS, $n = 10$) and obese (10 weeks old, KK 35.7 ± 1.4 g versus KKA^y 39.9 ± 1.0 g; $p < 0.05$, $n = 14$) male KKA^y mice to examine leptin-induced AMPK activation. The levels of AMPK and ACC phosphorylation were not significantly different between control KK and KKA^y mice at either age (Figures 3D–3G). Leptin i.c.v. led to a significant increase in AMPK (phospho-AMPK/AMPKα 90% ± 10% increase versus KK-vehicle; $p < 0.05$, $n = 5$) and ACC phosphorylation (125% ± 25% increase versus

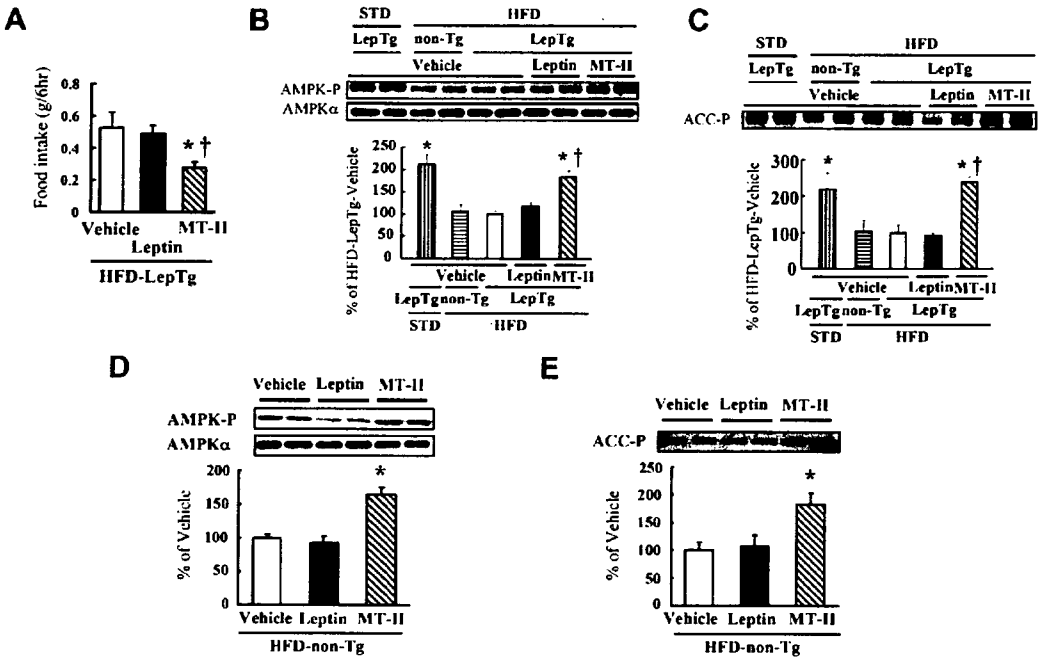

Figure 4. Recovery of Skeletal Muscle AMPK and ACC Phosphorylation by Intracerebroventricular MT-II Treatment in Mice Fed a High-Fat Diet

(A) Food intake over the 6 hr after i.c.v. injection in HFD-LepTg mice. *p < 0.05 versus vehicle, †p < 0.05 versus leptin, n = 7.

(B and D) Blots for phospho-AMPK and AMPKα, and graph showing phospho-AMPK/AMPKα ratio.

(C and E) Blots for phospho-ACC and quantified data.

(B–E) In HFD-LepTg mice, AMPK phosphorylation (B) and ACC phosphorylation (C) were decreased in comparison to STD-LepTg mice and were comparable to HFD-non-Tg mice. In HFD-LepTg mice, leptin i.c.v. did not alter AMPK (B) or ACC phosphorylation (C). MT-II (3.5 μg) i.c.v. restored AMPK (B) and ACC phosphorylation (C) in HFD-LepTg mice (*p < 0.05 versus HFD-LepTg-vehicle, †p < 0.05 versus HFD-LepTg-leptin, n = 7; data are % of HFD-LepTg vehicle) and HFD-non-Tg mice (D and E) (*p < 0.05 versus HFD-non-Tg-vehicle, n = 5).

KK-vehicle, $p < 0.05$, $n = 5$) in 6-week-old KK mice, while the increase was attenuated in 6-week-old KKA^y mice (phospho-AMPK/AMPKα 15% ± 21% increase, phospho-ACC 10% ± 11% increase; $p < 0.05$ versus KK-leptin, $n = 5$) (Figures 3D and 3E). ACC protein levels were not different between 6-week-old KK and KKA^y mice (Figure S1C). The results were similar in 10-week-olds, with a significant leptin-induced increase in AMPK (phospho-AMPK/AMPKα 85% ± 17% increase versus KK-vehicle; $p < 0.05$, $n = 7$) and ACC phosphorylation (133% ± 28% increase versus KK-vehicle; $p < 0.05$, $n = 7$) in KK mice and a lack of change in KKA^y mice by leptin (phospho-AMPK/AMPKα 18% ± 3% increase, phospho-ACC 21% ± 32% decrease; $p < 0.05$ versus KK-leptin, $n = 7$) (Figures 3F and 3G).

Central Treatment with MT-II Leads to Recovery of HFD-Induced Attenuation in AMPK and ACC Phosphorylation

LepTg mice exhibit decreased caloric intake and increased energy expenditure (Ogawa et al., 1999; Tanaka et al., 2005). Enhanced glucose tolerance, increased insulin sensitivity, and lower plasma triglyceride in LepTg mice are independent of reduced food intake (Ogawa et al., 1999). Over 4 weeks on HFD, LepTg mice, which remain significantly more hyperleptinemic than non-Tg mice (176 ± 4 versus 78 ± 7 ng/ml), become as obese, glucose intolerant, insulin resistant, and hyperlipidemic as non-Tg mice (Tanaka et al., 2005). Muscle AMPK/ACC phosphorylation is also attenuated (Tanaka et al., 2005).

To address the effect of central melanocortin activation under HFD, we treated HFD-LepTg mice with MT-II. MT-II i.c.v., but not leptin i.c.v., suppressed food intake in HFD-LepTg mice (vehicle 0.52 ± 0.10 g, leptin 0.49 ± 0.05 g, MT-II 0.28 ± 0.04 g; MT-II $p < 0.05$ versus vehicle or leptin, $n = 7$) (Figure 4A). In HFD-LepTg mice, muscle AMPK phosphorylation and ACC phosphorylation were significantly decreased compared with STD-LepTg mice and were comparable to HFD-non-Tg mice (Figures 4B and 4C). Of note, leptin i.c.v. in addition to transgenic hyperleptinemia did not augment AMPK (21% ± 14% increase, NS) or ACC phosphorylation (8% ± 6% decrease, NS) in HFD-LepTg mice (Figures 4B and 4C). In contrast, MT-II i.c.v. effectively augmented AMPK (by 85% ± 13%; $p < 0.05$ versus HFD-LepTg vehicle) and ACC phosphorylation (by 139% ± 16%; $p < 0.05$ versus HFD-LepTg vehicle) in HFD-LepTg mice (Figures 4B and 4C), suggesting that MT-II is a potent AMPK activator in muscle even under HFD. To confirm the results with LepTg mice, we treated HFD-fed wild-type (non-Tg) mice with leptin or MT-II

i.c.v. As expected, MT-II i.c.v., but not leptin i.c.v., led to a significant increase in muscle AMPK (leptin 8% ± 10% decrease, NS; MT-II 64% ± 12% increase versus vehicle; $p < 0.05$, $n = 5$) (Figure 4D) and ACC phosphorylation (leptin 19% ± 25% increase, NS; MT-II 96% ± 20% increase versus vehicle; $p < 0.05$, $n = 5$) (Figure 4E) in the wild-type mice. ACC expression was not altered by HFD or by HFD plus leptin or MT-II i.c.v. (Figure S1D).

DISCUSSION

Despite vigorous research, the question of why leptin loses its lipid-mobilizing potency under HFD has not been fully answered. Hypothalamic and peripheral induction of SOCS-3 (Bjorbaek et al., 1998; Howard et al., 2004; Wang et al., 2005; Kievit et al., 2006) and decreased permeability of the blood-brain barrier (El-Haschimi et al., 2000; Oh-I et al., 2005) have been implicated in attenuated leptin receptor signaling and metabolic efficacy. A recent study has demonstrated blunted hypothalamic AMPK as well as STAT3 signaling in HFD-fed mice (Martin et al., 2006). In the present study, neither transgenic hyperleptinemia nor central leptin treatment increased skeletal muscle AMPK phosphorylation under HFD. Notably, however, central MT-II administration did increase skeletal muscle AMPK phosphorylation in mice fed a HFD, indicating a mechanism upstream of the central melanocortin system that is responsible for the leptin resistance.

AMPK is a cellular fuel gauge activated by a variety of stresses. To stably assess AMPK activity in skeletal muscle, samples must be obtained quickly and deliberately. Furthermore, surgical interventions such as i.c.v. or intravenous cannulation cause substantial weight loss during the following week, making it more difficult to interpret the results in terms of energy homeostasis. In this sense, implementation of our devised protocol was instrumental in showing that skeletal muscle AMPK phosphorylation is regulated by the central melanocortin system. Phosphorylation of the α subunit of AMPK at Thr172 is tightly correlated with AMPK activity in many experimental conditions, including leptin-induced AMPK activation in the skeletal muscle (Minokoshi et al., 2002). Increased phosphorylation of AMPK and ACC in parallel firmly suggests increased AMPK activity in vivo.

In contrast to the effects of the central melanocortin system on satiety, little is known about its impact on fuel metabolism in the peripheral tissues. A recent study has shown that MT-II i.c.v. increases basal and insulin-stimulated glucose disposal and basal hepatic glucose production (Heijboer et al., 2005). However, MT-II does not seem to alter insulin-dependent suppression of hepatic glucose production (Heijboer et al., 2005). Our data here demonstrate that the administration of melanocortin agonist augments skeletal muscle AMPK and ACC phosphorylation. Considering the crucial role of skeletal muscle AMPK in the regulation of fatty acid β-oxidation (Minokoshi et al., 2002), our data strongly suggest a metabolic link between the central melanocortin system and skeletal muscle fatty acid mobilization. On the other hand, we did not observe any change in fasting plasma glucose or insulin levels 6 hr after MT-II i.c.v. Heijboer et al. (2005) also report an absence of change in basal plasma glucose and insulin levels following MT-II i.c.v. Further studies utilizing a combination of glucose clamp and measurement of AMPK activity may give a more accurate view of the temporal relationships between AMPK activation and skeletal muscle glucose utilization. POMC neurons are chiefly present in the ARC and NTS, while MC4R, a major melanocortin receptor involved in energy homeostasis, is widely distributed and present in the paraventricular hypothalamic nucleus (PVN) and the dorsal motor nucleus of the vagus (DMV) (Liu et al., 2003). Further studies are necessary to specify which nuclei within the central melanocortin system mediate skeletal muscle AMPK activation.

Leptin is a pleiotropic hormone, serving as a critical regulator of energy homeostasis, reproduction, blood pressure, and bone metabolism (Masuzaki et al., 1997; Aizawa-Abe et al., 2000; Ducy et al., 2000). Although a crucial role of the hypothalamic melanocortin system has been recognized in the anorexigenic effect of leptin, the matter of which functions of leptin are melanocortin dependent or independent still remains controversial. We previously reported that hypertension in LepTg mice is not ameliorated by SHU9119 i.c.v., implicating a melanocortin-independent pathway in blood pressure control by leptin (Aizawa-Abe et al., 2000). In terms of effects on glucose homeostasis, a recent study has shown that enhancement in hepatic gluconeogenesis by leptin is blocked by SHU9119 i.c.v., whereas leptin-dependent reduction in glycogenolysis is not (Gutierrez-Juarez et al., 2004). Taking these previous studjes together, it is reasonable to postulate that metabolic regulation by leptin is mediated by both melanocortin-dependent and -independent pathways. Here we show that pharmacological (SHU9119) or genetic (KKA^y) blockade of the melanocortin receptor attenuates leptin-dependent AMPK and ACC phosphorylation. These data provide evidence that the leptin-skeletal muscle AMPK axis is mediated by the central melanocortin system.

Leptin-induced augmentation of AMPK and ACC phosphorylation was attenuated in both 6-week-old and 10-week-old KKA^y mice. In 10-week-old obese KKA^y mice, decreased AMPK response to leptin may be partly attributable to the secondary effect of obesity. However, absence of muscle AMPK activation was observed even in lean 6-week-old KKA^y mice, further supporting the notion that melanocortin signaling is necessary for leptin-induced AMPK activation. In KKA^y mice, skeletal muscle phospho-AMPK levels were not altered compared with KK mice despite reported hyperphagia (Fan et al., 1997). Central administration of SHU9119 alone also causes hyperphagia (Fan et al., 1997) but did not alter skeletal muscle AMPK phosphorylation in our present study. The discrepancy between food intake and AMPK phosphorylation may suggest diverging pathways regulating satiety and skeletal muscle AMPK activity.

A recent study has shown that peripheral, but not central, administration of ciliary neurotrophic factor (CNTF), another potent anorectic agent in HFD-fed mice, activates

skeletal muscle AMPK (Watt et al., 2006). Although CNTF, like leptin, increases phospho-STAT3 in the ARC, the anorectic effect of CNTF remains intact in *Mc4r* knockout mice (Marsh et al., 1999). Noting that the anorectic effect of leptin is substantially attenuated in *Mc4r* knockouts (Marsh et al., 1999), these data suggest that central signaling cascades of leptin and CNTF are independent at the level of the melanocortin system and that centrally mediated AMPK activation in muscle is unique to the leptin-melanocortin pathway.

A previous work (Pierroz et al., 2002) and ours here demonstrate that MT-II suppresses food intake in mice fed a HFD. Another paper published recently has shown that leptin-induced α-MSH secretion from the ARC is abrogated in obese mice fed a HFD (Enriori et al., 2007). In the Enriori et al. study, the authors also showed that *Mc4r* expression is reciprocally upregulated in PVN from obese mice. These data further support our results showing that MT-II remains effective in suppressing food intake and activating skeletal muscle AMPK even under HFD. Taken together, our findings reinforce the notion that MT-II may be beneficial for the treatment of insulin resistance, a pathology characterized by a myocellular lipid excess. However, since the results of the present study are based mainly on data from i.c.v. injections, further studies are necessary to explore the clinical efficacy of melanocortin agonists.

In conclusion, our data demonstrate that leptin-induced skeletal muscle AMPK activation is at least partly mediated by the central melanocortin system. In contrast to leptin, AMPK activation by melanocortin agonist is preserved even under HFD. Our data provide an insight into the central regulation of skeletal muscle AMPK activity and suggest a possible recovery of skeletal muscle fatty acid β-oxidation by melanocortin agonists under dietary lipid overload.

EXPERIMENTAL PROCEDURES

Animal Experiments

C57BL/6 (B6), KK, and KKA^y mice were obtained from CLEA Japan. Heterozygous LepTg and non-Tg littermates on a B6 background (Ogawa et al., 1999) were used. Animals were maintained on STD (F-2, 3.7 kcal/g, 12% of kcal from fat, source soybean, Funahashi Farm) and a 14 hr light/10 hr dark cycle at 23°C. HFD was from Research Diets (D12493, 5.2 kcal/g, 60% of kcal from fat, source soybean/lard). Animals were given free access to food and water unless otherwise mentioned. Body weight and food intake were monitored for the animals' well-being. Experiments were started between 6 and 8 weeks of age, except for KK and KKA^y experiments. HFD was administered for 4 weeks. Cannulae (Plastics One) were inserted stereotactically into lateral ventricles and fixed. On the sampling day, leptin (0.5 μg), MT-II (3.5 μg), SHU9119 (1.0 μg), or a combination was administered in 0.5 μl saline solution at around the start of the light period. The weight of the food pellet at the start and at the end of the experiment was measured with a microbalance (A&D). Five to ten g/kg chloral hydrate (Nakalai Tesque) was administered through s.c. cannula (PE20, Becton Dickinson) 2 or 6 hr after i.c.v. injection, and the soleus muscle was sampled. Successful i.c.v. delivery of the reagents was ensured by injecting dye to every animal postmortem and omitting data from those with inadequate distribution of the dye. Plasma glucose and insulin levels were measured by Glucose C-II Test Wako (Wako Pure Chemical Industries) and Insulin ELISA Kit (Morinaga). Animal experiments were performed in accordance with the Kyoto University guidelines for animal experiments and were approved by the Animal Research Committee, Kyoto University Graduate School of Medicine.

Western Blots

Muscle samples were homogenized as described (Tanaka et al., 2005). After denaturing, 15 μg per lane of protein was loaded on 10% and 4%–20% SDS-polyacrylamide gels for AMPK and ACC, respectively, and transferred to PVDF membrane (PerkinElmer). Phosphospecific antibodies were used for the detection of phospho-AMPK and phospho-ACC. Antibodies were anti-phospho-Thr172 AMPKα, anti-AMPKα (Cell Signaling Technology), and anti-phospho-Ser79 ACC (Upstate). ECL Plus (Amersham), a LAS-1000 image analyzer, and MultiGauge version 2.0 (Fujifilm) were used for detection and quantification.

Statistical Analyses

Data are presented as means ± SEM. Comparisons between or among animal groups were performed by Student's t test or repeated analysis of variance (ANOVA), where applicable, and completed by Fisher's probable least-significant-difference test.

Supplemental Data

Supplemental Data include one figure and can be found with this article online at http://www.cellmetabolism.org/cgi/content/full/5/5/395/DC1/.

ACKNOWLEDGMENTS

We thank M. Nagamoto, S. Masumoto, K. Takahashi, S. Maki, K. Koyama, A. Yumoto, S. Kozuka, H. Managi, and K. Shiiya for assistance. This work was supported by MEXT Grants-in-Aid B2:16390267, S2:16109007, B:18790634, and adipomics:15081101; a MHLW Health and Labor Science Research Grant; and grants from JST, AstraZeneca, the Takeda Medical Research Foundation, the Smoking Research Foundation, Metabolic Syndrome Foundation, the Japan Foundation for Applied Enzymology, and NCVC.

Received: September 25, 2006
Revised: January 22, 2007
Accepted: April 17, 2007
Published: May 8, 2007

REFERENCES

Aizawa-Abe, M., Ogawa, Y., Masuzaki, H., Ebihara, K., Satoh, N., Iwai, H., Matsuoka, N., Hayashi, T., Hosoda, K., Inoue, G., et al. (2000). Pathophysiological role of leptin in obesity-related hypertension. J. Clin. Invest. *105*, 1243–1252.

Bjorbaek, C., Elmquist, J.K., Frantz, J.D., Shoelson, S.E., and Flier, J.S. (1998). Identification of SOCS-3 as a potential mediator of central leptin resistance. Mol. Cell *1*, 619–625.

Cowley, M.A., Smart, J.L., Rubinstein, M., Cerdan, M.G., Diano, S., Horvath, T.L., Cone, R.D., and Low, M.J. (2001). Leptin activates anorexigenic POMC neurons through a neural network in the arcuate nucleus. Nature *411*, 480–484.

Ducy, P., Amling, M., Takeda, S., Priemel, M., Schilling, A.F., Beil, F.T., Shen, J., Vinson, C., Rueger, J.M., and Karsenty, G. (2000). Leptin inhibits bone formation through a hypothalamic relay: a central control of bone mass. Cell *100*, 197–207.

Ebihara, K., Kusakabe, T., Hirata, M., Masuzaki, H., Miyanaga, F., Kobayashi, N., Tanaka, T., Chusho, H., Miyazawa, T., Hayashi, T., et al. (2007). Efficacy and safety of leptin-replacement therapy and possible mechanisms of leptin actions in patients with generalized lipodystrophy. J. Clin. Endocrinol. Metab. *92*, 532–541.

El-Haschimi, K., Pierroz, D.D., Hileman, S.M., Bjorbaek, C., and Flier, J.S. (2000). Two defects contribute to hypothalamic leptin resistance in mice with diet-induced obesity. J. Clin. Invest. *105*, 1827–1832.

Enriori, P.J., Evans, A.E., Sinnayah, P., Jobst, E.E., Tonelli-Lemos, L., Billes, S.K., Glavas, M.M., Grayson, B.E., Perello, M., Nillni, E.A., et al. (2007). Diet-induced obesity causes severe but reversible leptin resistance in arcuate melanocortin neurons. Cell Metab. *5*, 181–194.

Fan, W., Boston, B.A., Kesterson, R.A., Hruby, V.J., and Cone, R.D. (1997). Role of melanocortinergic neurons in feeding and the agouti obesity syndrome. Nature *385*, 165–168.

Farooqi, S.I., Keogh, J.M., Yeo, G.S.H., Lank, E.J., Gheetham, T., and O'Rahilly, S. (2003). Clinical spectrum of obesity and mutations in the melanocortin 4 receptor gene. N. Engl. J. Med. *348*, 1085–1095.

Gutierrez-Juarez, R., Obici, S., and Rossetti, L. (2004). Melanocortin-independent effects of leptin on hepatic glucose fluxes. J. Biol. Chem. *279*, 49704–49715.

Hardie, D.G., Hawley, S.A., and Scott, J.W. (2006). AMP-activated protein kinase- development of the energy sensor concept. J. Physiol. *574*, 7–15.

Heijboer, A.C., van den Hoek, A.M., Pijl, H., Voshol, P.J., Havekes, L.M., Romijn, J.A., and Corssmit, E.P. (2005). Intracerebroventricular administration of melanotan II increases insulin sensitivity of glucose disposal in mice. Diabetologia *48*, 1621–1626.

Howard, J.K., Cave, B.J., Oksanen, L.J., Tzameli, I., Bjorbaek, C., and Flier, J.S. (2004). Enhanced leptin sensitivity and attenuation of diet-induced obesity in mice with haploinsufficiency of Socs3. Nat. Med. *10*, 734–738.

Huszar, D., Lynch, C.A., Fairchild-Huntress, V., Dunmore, J.H., Fang, Q., Berkemeier, L.R., Gu, W., Kesterson, R.A., Boston, B.A., Cone, R.D., et al. (1997). Targeted disruption of the melanocortin-4 receptor results in obesity in mice. Cell *88*, 131–141.

Kievit, P., Howard, J.K., Badman, M.K., Balthasar, N., Coppari, R., Mori, H., Lee, C.E., Elmquist, J.K., Yoshimura, A., and Flier, J.S. (2006). Enhanced leptin sensitivity and improved glucose homeostasis in mice lacking suppressor of cytokine signaling-3 in POMC-expressing cells. Cell Metab. *4*, 123–132.

Kobayashi, H., Ogawa, Y., Shintani, M., Ebihara, K., Shimodahira, M., Iwakura, T., Hino, M., Ishihara, T., Ikekubo, K., Kurahachi, H., et al. (2002). A novel homozygous missense mutation of melanocortin-4 receptor (MC4R) in a Japanese woman with severe obesity. Diabetes *51*, 243–246.

Liu, H., Kishi, T., Roseberry, A.G., Cai, X., Lee, C.E., Montez, J.M., Friedman, J.M., and Elmquist, J.K. (2003). Transgenic mice expressing green fluorescent protein under the control of the melanocortin-4 receptor promoter. J. Neurosci. *23*, 7143–7154.

Lu, D., Willard, D., Patel, I.R., Kadwell, S., Overton, L., Kost, T., Luther, M., Chen, W., Woychik, R.P., Wilkison, W.O., et al. (1994). Agouti protein is an antagonist of the melanocyte-stimulating-hormone receptor. Nature *371*, 799–802.

Maffei, M., Halaas, J., Ravussin, E., Pratley, R.E., Lee, G.H., Zhang, Y., Fei, H., Kim, S., Lallone, R., Ranganathan, S., et al. (1995). Leptin levels in human and rodent: Measurement of plasma leptin and ob RNA in obese and weight-reduced subjects. Nat. Med. *1*, 1155–1161.

Marsh, D.J., Hollopeter, G., Huszar, D., Laufer, R., Yagaloff, K.A., Fisher, S.L., Burn, P., and Palmiter, R.D. (1999). Response of melanocortin-4 receptor-deficient mice to anorectic and orexigenic peptides. Nat. Genet. *21*, 119–122.

Martin, T.L., Alquier, T., Asakura, K., Furukawa, N., Preitner, F., and Kahn, B.B. (2006). Diet-induced obesity alters AMP kinase activity in hypothalamus and skeletal muscle. J. Biol. Chem. *281*, 18933–18941.

Masuzaki, H., Ogawa, Y., Sagawa, N., Hosoda, K., Matsumoto, T., Mise, H., Nishimura, H., Yoshimasa, Y., Tanaka, I., Mori, T., et al. (1997). Nonadipose tissue production of leptin: leptin as a novel placenta-derived hormone in humans. Nat. Med. *3*, 1029–1033.

Minokoshi, Y., Kim, Y.B., Peroni, O.D., Fryer, L.G., Muller, C., Carling, D., and Kahn, B.B. (2002). Leptin stimulates fatty-acid oxidation by activating AMP-activated protein kinase. Nature *415*, 339–343.

Ogawa, Y., Masuzaki, H., Hosoda, K., Aizawa-Abe, M., Suga, J., Suda, M., Ebihara, K., Iwai, H., Matsuoka, N., Satoh, N., et al. (1999). Increased glucose metabolism and insulin sensitivity in transgenic skinny mice overexpressing leptin. Diabetes *48*, 1822–1829.

Oh-I, S., Shimizu, H., Sato, T., Uehara, Y., Okada, S., and Mori, M. (2005). Molecular mechanisms associated with leptin resistance: n-3 polyunsaturated fatty acids induce alterations in the tight junction of the brain. Cell Metab. *1*, 331–341.

Oral, E.A., Simha, V., Ruiz, E., Andewelt, A., Premkumar, A., Snell, P., Wagner, A.J., Depaoli, A.M., Reitman, M.L., Taylor, S.I., et al. (2002). Leptin-replacement therapy for lipodystrophy. N. Engl. J. Med. *346*, 570–578.

Pierroz, D.D., Ziotopoulou, M., Ungsunan, L., Moschos, S., Flier, J.S., and Mantzoros, C.S. (2002). Effects of acute and chronic administration of the melanocortin agonist MTII in mice with diet-induced obesity. Diabetes *51*, 1337–1345.

Schwartz, M.W., Seeley, R.J., Woods, S.C., Weigle, D.S., Campfield, L.A., Burn, P., and Baskin, D.G. (1997). Leptin increases hypothalamic pro-opiomelanocortin mRNA expression in the rostral arcuate nucleus. Diabetes *46*, 2119–2123.

Seeley, R.J., Yagaloff, K.A., Fisher, S.L., Burn, P., Thiele, T.E., van Dijk, G., Baskin, D.G., and Schwartz, M.W. (1997). Melanocortin receptors in leptin effects. Nature *390*, 349.

Shimabukuro, M., Koyama, K., Chen, G., Wang, M.Y., Trieu, F., Lee, Y., Newgard, C.B., and Unger, R.H. (1997). Direct antidiabetic effect of leptin through triglyceride depletion of tissues. Proc. Natl. Acad. Sci. USA *94*, 4637–4641.

Tanaka, T., Hidaka, S., Masuzaki, H., Yasue, S., Minokoshi, Y., Ebihara, K., Chusho, H., Ogawa, Y., Toyoda, T., Sato, K., et al. (2005). Skeletal muscle AMP-activated protein kinase phosphorylation parallels metabolic phenotype in leptin transgenic mice under dietary modification. Diabetes *54*, 2365–2374.

Wang, M.Y., Orci, L., Ravazzola, M., and Unger, R.H. (2005). Fat storage in adipocytes requires inactivation of leptin's paracrine activity: implications for treatment of human obesity. Proc. Natl. Acad. Sci. USA *102*, 18011–18016.

Watt, M.J., Dzamko, N., Thomas, W.G., Rose-John, S., Ernst, M., Carling, D., Kemp, B.E., Febbraio, M.A., and Steinberg, G.R. (2006). CNTF reverses obesity-induced insulin resistance by activating skeletal muscle AMPK. Nat. Med. *12*, 541–548.

Available online at www.sciencedirect.com

ScienceDirect

Metabolism Clinical and Experimental 56 (2007) 1719–1728

Metabolism
Clinical and Experimental

www.elsevier.com/locate/metabol

High-fat diet impairs the effects of a single bout of endurance exercise on glucose transport and insulin sensitivity in rat skeletal muscle

Satsuki Tanaka[a], Tatsuya Hayashi[a,b,*], Taro Toyoda[c], Taku Hamada[b], Yohei Shimizu[b], Masakazu Hirata[a], Ken Ebihara[a], Hiroaki Masuzaki[a], Kiminori Hosoda[a], Tohru Fushiki[c], Kazuwa Nakao[a]

[a]*Department of Medicine and Clinical Science, Graduate School of Medicine, Kyoto University, Kyoto 606-8507, Japan*
[b]*Laboratory of Sports and Exercise Medicine, Graduate School of Human and Environmental Studies, Kyoto University, Kyoto 606-8501, Japan*
[c]*Laboratory of Nutrition Chemistry, Division of Food Science and Biotechnology, Graduate School of Agriculture, Kyoto University, Kyoto 606-8502, Japan*

Received 4 May 2007; accepted 10 July 2007

Abstract

A single bout of exercise increases the rate of muscle glucose transport (GT) by both insulin-independent and insulin-dependent mechanisms. The purpose of this study was to determine whether high-fat diet (HFD) feeding interferes with the metabolic activation induced by moderate-intensity endurance exercise. Rats were fed an HFD or control diet (CD) for 4 weeks and then exercised on a treadmill for 1 hour (19 m/min, 15% incline). Insulin-independent GT was markedly higher in soleus muscle dissected immediately after exercise than in muscle dissected from sedentary rats in both dietary groups, but insulin-independent GT was 25% lower in HFD-fed than in CD-fed rats. Insulin-dependent GT in the presence of submaximally effective concentration of insulin (0.9 nmol/L) was also higher in both dietary groups in muscle dissected 2 hours after exercise, but was 25% lower in HFD-fed than in CD-fed rats. Exercise-induced activation of 5′adenosine monophosphate–activated protein kinase, a signaling intermediary leading to insulin-independent GT and regulating insulin sensitivity, was correspondingly blunted in the HFD group. High-fat diet did not affect glucose transporter 4 content or insulin-stimulated Akt phosphorylation. Our findings provide evidence that an HFD impairs the effects of short-term endurance exercise on glucose metabolism and that exercise does not fully compensate for HFD-induced insulin resistance in skeletal muscle. Although the underlying mechanism is unclear, reduced 5′adenosine monophosphate–activated protein kinase activation during exercise may play a role.

1. Introduction

Physical exercise has profound effects on glucose metabolism in contracting skeletal muscle. Exercise activates glucose transport (GT) in skeletal muscle by inducing translocation of glucose transporter 4 (GLUT4) to the cell surface by insulin-independent and insulin-dependent mechanisms (reviewed in Hayashi et al [1]). The activity of insulin-independent GT is markedly enhanced during exercise; and this effect wears off within several hours after exercise, when the postexercise increase in insulin sensitivity that leads to insulin-dependent GT becomes prominent. Wallberg-Henriksson et al [2] showed in isolated rat skeletal muscle that the rate of insulin-independent GT is maximal immediately after exercise, whereas the postexercise increase in insulin sensitivity becomes detectable 3 hours after exercise. Correspondingly, Price et al [3] showed in human muscle that postexercise glycogen repletion occurs in an insulin-independent manner for about 1 hour after exercise, after which insulin-dependent glycogen repletion becomes significant. These exercise-stimulated mechanisms form the basis of practices to prevent individuals from developing glucose intolerance and to improve glycemic control in patients with type 2 diabetes mellitus.

It is of interest to know whether exercise-stimulated GT, including both the insulin-independent and insulin-dependent components, is normal in the state of insulin resistance. Although numerous studies have shown that a

* Corresponding author. Laboratory of Sports and Exercise Medicine, Graduate School of Human and Environmental Studies, Kyoto University, Yoshida-nihonmatsu-cho, Sakyo-ku, Kyoto, 606-8501, Japan. Tel.: +81 75 753 6640; fax: +81 75 753 6640.
E-mail address: tatsuya@kuhp.kyoto-u.ac.jp (T. Hayashi).

0026-0495/$ – see front matter © 2007 Elsevier Inc. All rights reserved.
doi:10.1016/j.metabol.2007.07.017

high-fat diet (HFD) causes insulin resistance in muscles at rest, it is unknown whether an HFD interferes with the short-term stimulatory effect of exercise on insulin sensitivity. Only one study has addressed this topic and demonstrated that the postexercise increase in muscle insulin sensitivity is abolished completely in HFD-fed rats [4]. In that study, however, insulin-dependent GT was measured before the insulin-independent glucose uptake wore off (its activity was still 160% higher than the basal uptake), indicating that the net effect of exercise on insulin sensitivity was substantially underestimated because of residual glucose uptake activity. There is considerable controversy over whether an HFD alters the effects of short-term exercise on insulin-independent GT. Most investigators have reported about 50% reduction in the rate of muscle GT stimulated by exercise [5-7] and electrical stimulation [6,8,9] in HFD-fed rodents, although others did not find these effects [4,10]. Moreover, some studies have shown that the reduction in insulin-independent GT was not associated with decreased muscle GLUT4 content [5,6]; but a conflicting result was also reported [8]. Although Hansen et al [9] showed that impairment of the exercise-stimulated GT is associated with decreased GLUT4 translocation to the cell surface, the responsible signaling mechanism remains to be elucidated.

The purposes of our present study were to determine how HFD affects insulin-independent and insulin-dependent GT activated by a single bout of endurance exercise and to explore the underlying mechanism that leads to the change in exercise-stimulated glucose utilization. We found that both components of exercise-induced GT were impaired by an HFD and that these changes were accompanied by a decrease in 5′adenosine monophosphate (AMP) activated protein kinase (AMPK) activation in skeletal muscle of rats fed an HFD for 4 weeks.

2. Materials and methods

2.1. Animals and diets

Male Wistar rats at the time of weaning were purchased from Clea Japan (Tokyo, Japan). Animals were fed either control diet (CD) (MF: 3.6 kcal/g, 12% kcal fat, source: soybean: Oriental Yeast, Tokyo, Japan) or HFD (D12493: 5.2 kcal/g, 60% kcal fat, source: soybean/lard: Research Diets, New Brunswick, NJ) for 4 weeks. All animal experiments were approved by the Animal Research Committee, Graduate School of Medicine, Kyoto University.

2.2. Exercise and muscle sampling

The rats were accustomed to a rodent treadmill (Muromachi Kikai, Kyoto, Japan) by running at 14 to 18 m/min on a 15% grade for 5 minutes on the day before the experiment. After an overnight fast, rats performed treadmill running at 19 m/min on a 15% grade for 1 hour or were kept sedentary. To study insulin-independent GT, exercised rats were killed by cervical dislocation immediately after the cessation of running; and the soleus muscles were isolated. Muscles were incubated in 7 mL Krebs-Ringer bicarbonate buffer containing 2 mmol/L pyruvate (KRBP) at 37°C for 20 minutes, and then 3-*O*-methyl-D-glucose (3MG) uptake activity was determined as described previously [11-14]. Muscles dissected from sedentary rats were treated similarly. Some of the muscles were frozen in liquid nitrogen immediately after dissection for analysis of isoform-specific AMPK activity and Western blotting of phosphorylated AMPKα and phosphorylated acetyl-coenzyme A carboxylase (ACC). Muscles from sedentary animals were also analyzed by Western blotting of total AMPKα and GLUT4. For histochemical analysis, soleus muscles were isolated from sedentary animals and frozen in dry ice-cooled 2-methylbutane. Abdominal fat (epididymal, retroperitoneal, and mesenteric fat pads) was collected from sedentary animals and weighed. To study the postexercise effect on insulin-dependent GT, exercised and sedentary rats were placed in separate cages with free access to drinking water but without food for 2 hours, after which the rats were killed by cervical dislocation and the soleus muscles were dissected. Isolated muscles were incubated for 30 minutes in KRBP in the absence or presence of half-maximally effective insulin (0.9 nmol/L) at 37°C, and then 3MG uptake was determined. Some muscles were frozen in liquid nitrogen immediately after incubation for Western blotting of phosphorylated Akt, a signaling intermediary leading to insulin-stimulated GT. To measure glycogen and triglyceride content, muscles were isolated from sedentary rats and from exercised rats immediately and 2 hours after exercise, and frozen in liquid nitrogen. We chose soleus muscle because our preliminary studies showed that soleus muscle provided the most prominent activation of insulin-independent and insulin-dependent GT in response to exercise compared with other muscles including extensor digitorum longus and epitrochlearis.

2.3. 3MG uptake

To assay GT, incubated muscles were transferred to 2 mL Krebs-Ringer bicarbonate buffer containing 1 mmol/L 3-*O*-[methyl-^{3}H]-D-glucose (1.5 μCi/mL) (American Radiolabeled Chemicals, St Louis, MO) and 7 mmol/L D-[^{14}C] mannitol (0.3 μCi/mL) (PerkinElmer Life Science, Boston, MA) at 30°C and incubated for 10 minutes [11-14]. The muscles were weighed and processed by incubating them in 450 μL of 1 mol/L NaOH at 80°C for 10 minutes. Digestates were neutralized with 1 mol/L HCl, and particulates were precipitated by centrifugation at 20000*g* for 2 minutes. Radioactivity in aliquots of the digested protein was determined by liquid scintillation counting for dual labels.

2.4. Isoform-specific AMPK activity assay

Muscles were treated as described [11-14]. Frozen muscles were homogenized in ice-cold lysis buffer (1:40

wt/vol) containing 20 mmol/L Tris-HCl (pH 7.4), 1% Triton X-100, 50 mmol/L NaCl, 250 mmol/L sucrose, 50 mmol/L NaF, 5 mmol/L sodium pyrophosphate, 2 mmol/L dithiothreitol, 4 mg/L leupeptin, 50 mg/L soybean trypsin inhibitor, 0.1 mmol/L benzamidine, and 0.5 mmol/L phenylmethylsulfonyl fluoride, and centrifuged at 14000*g* for 30 minutes at 4°C. The supernatants (100 μg of protein) were immunoprecipitated with antibodies directed against the α1 or α2 catalytic subunits of AMPK [11] and protein A–Sepharose CL-4B (Amersham, Buckinghamshire, United Kingdom). Kinase reactions were performed in the presence of SAMS peptide [11], and then ^{32}P incorporation was quantitated with a scintillation counter.

2.5. Western blotting

For analysis of phosphorylated AMPKα, total AMPKα, phosphorylated ACC, and phosphorylated Akt, muscles were homogenized in lysis buffer used for isoform-specific AMPK activity. Lysates were solubilized in Laemmli sample buffer containing mercaptoethanol and boiled. For analysis of GLUT4, muscles were homogenized in ice-cold buffer containing 250 mmol/L sucrose, 20 mmol/L 2-[4-(2-hydroxyethyl)-1-piperadinyl] ethonsulforic acid (HEPES) (pH 7.4), and 1 mmol/L EDTA, and centrifuged at 1200*g* for 5 minutes. The supernatant was centrifuged at 200 000*g* for 60 minutes at 4°C. The resulting pellet was solubilized in Laemmli sample buffer containing dithiothreitol. Samples were subjected to sodium dodecyl sulfate polyacrylamide gel electrophoresis, and proteins were transferred to polyvinylidene difluoride membranes (PolyScreen; PerkinElmer, Wellesley, MA). Blocked membranes were incubated with phosphospecific AMPKα Thr^{172} (Cell Signaling Technology, Beverly, MA), total AMPKα (Cell Signaling Technology), phosphospecific ACC Ser^{79} (Upstate Biotechnology, Lake Placid, NY), phosphospecific Akt (Ser^{473}) (Cell Signaling Technology), and GLUT4 (Biogenesis; South Coast, United Kingdom) antibodies. Proteins were visualized with enhanced chemiluminescence reagents (Amersham). The signal was quantified with a Lumino-Image Analyzer LAS-1000 System (Fuji Photo Film, Tokyo, Japan).

2.6. Histochemical analysis

Serial sections (10 μm thick) were used for muscle fiber typing and intramyocellular lipid (IMCL) measurement. To determine muscle fiber type (type I, IIa), myosin adenosine triphosphatase (ATPase) staining was performed as described [15,16]. Sections were incubated in acidic (30 mmol/L sodium barbital and 50 mmol/L sodium acetate, adjusted to pH 4.3 with HCl) or alkaline buffer (50 mmol/L $CaCl_2$ and 75 mmol/L NaCl, adjusted to pH 10.6 with NaOH) and then incubated in staining buffer (2.8 mmol/L adenosine triphosphate, 50 mmol/L $CaCl_2$, 75 mmol/L NaCl, adjusted to pH 9.4 with NaOH), followed by immersion in 1% $CaCl_2$, 2% $CoCl_2$, and 1% $(NH_4)_2S$. The sections were treated in ethanol and xylol, dried in the air, and then mounted with Aquatex (Merk, Darmstadt, Germany). Fiber type distribution was determined by counting the number of each fiber type in 100 contiguous fibers in a muscle section. To determine IMCL content, the oil red O (ORO) staining procedure and stained area measurement were performed as described [17]. Sections were incubated with formaldehyde-methanol (1:1 vol/vol) and then incubated with ORO solution followed by extensive wash with distilled water. The sections were dried in the air and then mounted with Aquatex. Images from each section were saved as gray-scale images, and the digitized data were then analyzed using the freeware ImageJ software (http://rsb.info.nih.gov/). The amount of IMCL in each fiber was quantified as the percentage of the area occupied by ORO-stained droplets (total area occupied by lipid droplets of a muscle fiber) × 100/total cross-sectional area of the fiber. Lipid area was calculated for each of 3 different fields within the section, and a mean percentage was then calculated for each muscle [17].

2.7. Muscle glycogen and triglyceride content measurement

Glycogen content was assayed as described [12,14]. Frozen muscles were weighed and digested in 1 mol/L NaOH (1:9 wt/vol) at 80°C for 10 minutes. The digestates were neutralized with 1 mol/L HCl, and then 6 mol/L HCl was added to obtain a final concentration of 2 mol/L HCl. The digestates were incubated at 85°C for 2 hours and then neutralized with 5 mol/L NaOH. The concentration of hydrolyzed glucose residues was measured enzymatically using the hexokinase glucose assay reagent (Glucose CII Test; Wako, Osaka, Japan). Triglyceride content was measured as described [18]. Total lipids were extracted from muscles with isopropyl alcohol–heptane (1:1 vol/vol) and saponified in ethanolic KOH (0.5 mol/L). Free glycerol concentration was then determined using a commercial kit (Triglyceride E Test; Wako).

2.8. Blood sample analysis

Blood samples were collected from the tail vein using heparinized glass tube 3 days before the experimental day after an overnight fast. Plasma levels for glucose (Glutest-Ace; Sanwa Kagaku Kenkyusyo, Nagoya, Japan), insulin (rat insulin ELISA kit; Morinaga, Yokohama, Japan), leptin (rat leptin radioimmunoassay kit; LINCO, St Charles, MO), triglycerides (Triglyceride E Test; Wako), and lactate (Lactate Pro; Arkray, Kyoto, Japan) were measured. Lactate concentration was also measured on the experimental day immediately after exercise.

2.9. Statistical analysis

Results are presented as means ± SE. The significance of difference between 2 groups was evaluated using Student *t* test. Multiple means were compared by analysis of variance followed by post hoc analysis using Dunn's procedure. $P < .05$ was considered statistically significant.

3. Results

3.1. Metabolic parameters in rats fed the CD and HFD

Table 1 summarizes the basic characteristics of the CD- and HFD-fed rats (Table 1). Rats fed the HFD for 4 weeks were slightly heavier and had higher plasma concentrations of glucose, insulin, triglycerides, and leptin than did CD-fed rats.

3.2. HFD increases IMCL in soleus

We analyzed the influence of HFD on IMCL concentration by ORO staining (Fig. 1A-B). Muscle fiber type was determined by myofibrillar ATPase histochemical staining (Fig. 1C-F). The fiber type proportions did not differ significantly between CD-fed and HFD-fed rats (CD, 80.7% ± 1.2% type I and 19.3% ± 1.2% type IIa fibers; HFD, 79.2% ± 2.5% type I and 20.8% ± 2.5% type IIa fibers). In both muscle fiber types, the IMCL content in HFD-fed rat muscle was twice as high as that in muscles from CD-fed rats. In CD-fed rats, the IMCL content was 2.3% ± 0.5% in type I fibers and 5.9% ± 1.3% in type IIa fibers. In HFD-fed rats, the respective values were 4.5% ± 0.9% and 12.8% ± 2.0% ($P < .05$ vs CD) (Fig. 1G). The IMCL content in the total soleus muscle was also twice as high in the HFD group than in the CD group (3.0% ± 0.7% vs 6.2% ± 1.0%, $P < .05$) (Fig. 1G).

3.3. HFD attenuates activation of insulin-independent GT induced by one bout of endurance exercise

To analyze insulin-independent GT stimulated by one bout of exercise, soleus muscles were dissected and 3MG uptake was determined ex vivo in the absence of insulin immediately after exercise (Fig. 2). Exercise elicited significant activation of insulin-independent 3MG uptake by 3.4 times in muscles from CD-fed rats and by 2.9 times in muscles from HFD-fed rats. However, the rate of insulin-independent 3MG uptake stimulated by exercise was 25% lower in muscles from HFD-fed rats (0.15 ± 0.02 μmol/[g h]) than in muscles from CD-fed rats (0.11 ± 0.01 μmol/[g h]) ($P < .05$). Basal glucose uptake was not affected by dietary manipulation.

Table 1
Metabolic parameters in rats under HFD and CD feeding

	CD	HFD
Body weight (g)	193 ± 2	203 ± 3*
Food intake (kcal/d)	54 ± 1	58 ± 1*
Plasma glucose (mg/dL)	78 ± 2	88 ± 2*
Plasma insulin (mg/dL)	1.3 ± 0.1	2.5 ± 0.2*
Plasma triglycerides (mg/dL)	98 ± 4	122 ± 8*
Plasma leptin (ng/mL)	1.6 ± 0.2	7.6 ± 0.4*
Abdominal fat (g)	5.3 ± 0.5	9.7 ± 0.4*

Male Wistar rats at the time of weaning were fed CD or HFD for 4 weeks. Body weight, abdominal fat weight, and plasma parameters were measured at the end of week 4. Blood samples were obtained after an overnight fast at 9:00 to 11:00 AM. Data are means ± SE; n = 6 to 19 per group.

* $P < .05$ vs CD-fed group.

3.4. One bout of endurance exercise activates insulin-dependent GT after exercise, but does not fully compensate for insulin resistance in muscle from HFD-fed rats

The effect of the HFD on insulin-dependent GT is shown in Fig. 3. The rate of insulin-dependent 3MG uptake was 59% lower in muscles from sedentary HFD-fed rats than in sedentary CD-fed rats (0.12 ± 0.02 vs 0.05 ± 0.01 μmol/[g h], $P < .05$), indicating marked insulin resistance in the HFD-fed animals (Fig. 3; insulin+, sedentary). Two hours after exercise, when insulin-independent 3MG uptake stimulated by exercise had declined significantly (Fig. 3; insulin−, 2 hours postexercise), insulin-dependent 3MG uptake was markedly higher in muscles from exercised animals than in muscles from sedentary rats in both dietary groups (Fig. 3; insulin+, 2 hours postexercise). The net increase in the rate of insulin-stimulated 3MG uptake was similar in both dietary groups (CD, 0.33 ± 0.03 μmol/[g h] vs HFD, 0.27 ± 0.02 μmol/[g h]). However, the rate of insulin-stimulated 3MG uptake was still 25% lower in HFD-fed rats than in CD-fed rats (0.36 ± 0.03 vs 0.27 ± 0.03 μmol/[g h], $P < .05$).

3.5. HFD attenuates muscle AMPKα2 activation by one bout of endurance exercise

We evaluated whether the HFD affects muscle AMPK activity, a signaling intermediary leading to insulin-independent GT [12,19-21] and regulation of insulin sensitivity [22-24]. Neither diet nor one bout of exercise had an effect on AMPKα1 activity (Fig. 4A). In contrast, exercise increased AMPKα2 activity by 1.6 times in muscle from CD-fed rats ($P < .05$), whereas in muscle from HFD-fed rats, AMPKα2 activation did not change significantly (Fig. 4B). Interestingly, the basal AMPKα2 activity was 1.3 times higher in muscle from HFD-fed rats than from CD-fed rats ($P < .05$), whereas the AMPKα2 activity immediately after exercise was similar in both dietary groups (Fig. 4B). Therefore, the exercise-mediated response of AMPKα2 activity was significantly lower in HFD-fed than in CD-fed rats. This is consistent with the findings of AMPKα2 activity: exercise increased phosphorylation of the Thr172 residue of AMPKα, an essential site for full kinase activation (Fig. 4C), and the Ser79 residue of ACC, a known substrate of muscle AMPK (Fig. 4D), in muscles from CD-fed animals, but not in HFD-fed animals. The protein level of AMPKα did not differ between muscles from both dietary groups (Fig. 4E).

3.6. One bout of endurance exercise dose not affect insulin-stimulated phosphorylation of muscle Akt in CD- and HFD-fed rats

To determine whether HFD impairs the downstream of phosphatidylinositol 3-kinase (PI-3 kinase), we measured the

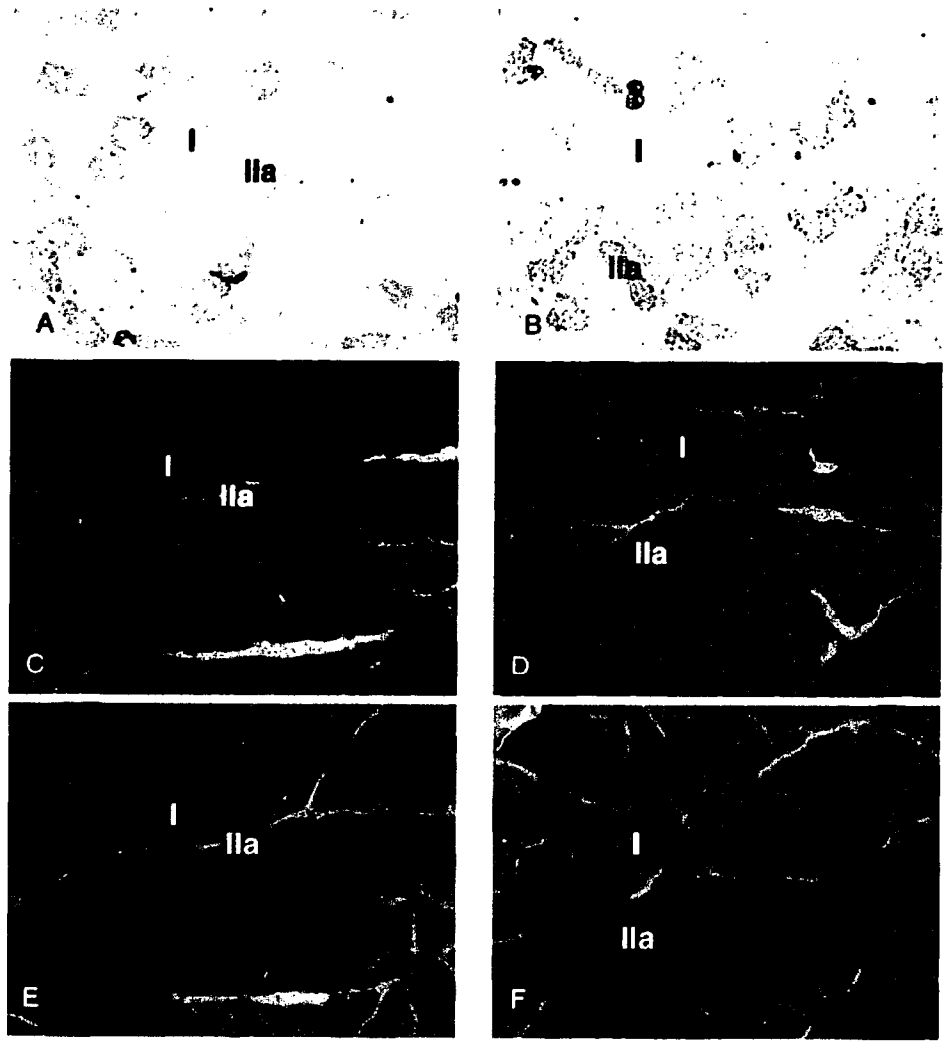

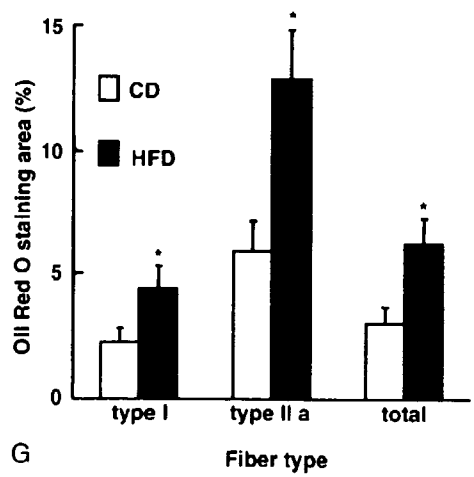

Fig. 1. High-fat diet increases IMCL content in soleus muscle. Representative transverse sections of soleus muscle dissected from CD-fed (A, C, and E) and HFD-fed (B, D, and F) rats (80× magnification). A and B, Oil red O staining of IMCL. Oil red O stains neutral lipid (mainly triglycerides) with an orange-red tint, and lipid droplets are seen as distinct spots of stain (A, B). C and D, Myosin ATPase staining (pH 4.3). Light and dark fibers are type IIa and I, respectively (C, D). E and F, Myosin ATPase staining (pH 10.6). Light and dark fibers are type I and IIa, respectively (E, F). G, Fiber type–specific IMCL content, expressed as a percentage of the area of lipid stained. Data are means ± SE; n = 7 per group. *$P < .05$ vs CD-fed group.